7618 J. Med. Chem. 2009, 52, 7618–7630
DOI: 10.1021/jm9005127

Journal of Medicinal Chemistry Article

3,4-Diaryl-isoxazoles and -imidazoles as Potent Dual Inhibitors of p38α Mitogen Activated Protein Kinase and Casein Kinase 1δ†

Christian Peifer,*[,‡,∥] Mohammed Abadleh,[‡] Joachim Bischof,[§] Dominik Hauser,[‡,⊥] Verena Schattel,[‡] Heidrun Hirner,[§] Uwe Knippschild,[§] and Stefan Laufer[‡]

[‡]*Department of Pharmacy, Eberhard-Karls-University, Auf der Morgenstelle 8, D-72076 Tuebingen, Germany,* [§]*Department of General, Visceral and Transplantation Surgery, Surgery Centre, University of Ulm, Steinhoevelstrasse 9, D-89075 Ulm, Germany,* [∥]*MRC Protein Phosphorylation Unit, School of Life Sciences, MSI/WTB Complex, University of Dundee, Dow Street, Dundee DD1 5EH, Scotland/U.K., and* [⊥]*c-a-i-r biosciences GmbH, Paul-Ehrlich-Strasse 15, 72076 Tuebingen, Germany*

Received April 22, 2009

In this study, we report on the discovery of isoxazole **1** as a potent dual inhibitor of p38α (IC_{50} = 0.45 μM) and CK1δ (IC_{50} = 0.23 μM). Because only a few effective small molecule inhibitors of CK1 have been described so far, we aimed to develop this structural class toward specific agents. Molecular modeling studies comparing p38α/CK1δ suggested an optimization strategy leading to design, synthesis, biological characterization, and SAR of highly potent compounds including **9** (IC_{50} p38α = 0.006 μM; IC_{50} CK1δ = 1.6 μM), **13** (IC_{50} p38α = 2.52 μM; IC_{50} CK1δ = 0.033 μM), **17** (IC_{50} p38α = 0.019 μM; IC_{50} CK1δ = 0.004 μM; IC_{50} CK1ε = 0.073 μM), and **18** (CKP138) (IC_{50} p38α = 0.041 μM; IC_{50} CK1δ = 0.005 μM; IC_{50} CK1ε = 0.447 μM) possessing differentiated specificity. Selected compounds were profiled over 76 kinases and evaluation of their cellular efficacy showed **18** (CKP138) to be a highly potent and dual-specific inhibitor of CK1δ and p38α.

Introduction

Small molecule inhibitors of various protein kinases are utilized extensively in research and drug development. The human kinome consists of more than 500 protein kinases, and kinase inhibitors typically bind in the highly conserved ATP pocket of these enzymes.[1] Thus the specificity of ATP competitive kinase inhibitors is of significant interest and represents a crucial factor for their use in, e.g., signal transduction research or therapeutic applications. Recently, we reported on the substituted isoxazoles **1** and **2** (Table 1), which have been originally designed and characterized as ATP competitive p38α mitogen activated protein kinase (MAPK[a]) inhibitors (IC_{50} p38α MAPK **1** = 0.45 μM and **2** = 2.2 μM).[2,3] These compounds possess the typical vicinal pyridin-4-yl/4-*F*-phenyl pharmacophore of first generation p38α MAPK inhibitors. The well characterized p38α MAPK is deemed to be a key player in the signal transduction of severe diseases such as rheumatoid arthritis, asthma, and autoimmune disorders and is considered to be a validated drug target for anti-inflammatory agents.[4] However, profiling compounds **1** and **2** in a panel of 78 protein kinases at a concentration of 10 μM also revealed significant inhibition of casein kinase 1 δ (CK1δ) for **1** (90% inhibition), while its isomer **2** was less potent (CK1δ 40% inhibition, Table 1). Subsequently, **1** was determined to inhibit CK1δ with an IC_{50} value of 0.23 μM. Furthermore, in this panel, JNK2 and JNK3 were slightly less potently inhibited by **1** (JNK2 87% inhibition at 10 μM, IC_{50} = 1.28 μM; JNK3 72% inhibition at 10 μM, IC_{50} = 0.54 μM). These results were in line with data from recent studies, which identified classical p38α MAPK inhibitors such as **19** and **20** sharing the same pharmacophore moiety as **1** being able to inhibit CK1δ (e.g., **19**: CK1δ 92% inhibition at 1 μM, IC_{50} = 0.12 μM, Scheme 1).[5−7] Hence, we became interested

† Contribution to celebrate the 100th anniversary of the Division of Medicinal Chemistry of the American Chemical Society.

*To whom correspondence should be addressed. Correspondence to: Phone: 0049 7071 29 75278. Fax: 0049 7071 29 5037. E-mail: Christian.Peifer@uni-tuebingen.de.

[a] Abbreviations: AMPK, 5′AMP activated protein kinase; BRSK2, BR serine-threonine kinase-2; BTK, Bruton agammaglobulinemia protein kinase; CAMK1, Ca^{2+}/calmodulin-dependent kinase; CAMKKb, Ca^{2+}/calmodulin-dependent kinase kinase β; CDK, cyclin dependent protein kinase; CHK, cell cycle checkpoint kinase; CK, casein kinase; CSK, C-terminal Src kinase; DYRK, dual-specificity tyrosine-phosphorylated and -regulated kinase; EF2K, elongation factor 2 kinase; EPH A2, epithelial cell kinase; ERK, mitogen activated protein kinase 1; FGF-R1, fibroblast growth factor receptor 1; GSK3, glycogen synthase kinase 3; HIPK2, homeodomain interacting protein kinase 2; HP, hydrophobic pocket; HR, hydrophobic region; IGF, insulin-like growth factor; IGF-1R, insulin-like growth factor 1 receptor; IKKb, I-κ-B-kinase β; IRR, insulin receptor-related receptor; JNK, c-Jun N-terminal kinase; kd, kinase domain; Lck, lymphocyte-specific protein tyrosine kinase; MAPK, mitogen activated protein kinase; MAPKAP-K2, MAPK activated protein kinase-2; MARK, microtubule affinity regulating kinase; MELK, maternal embryonic leucine zipper kinase; MKK1, MAPK kinase-1; MNK, MAPK interacting kinase; MSK1, mitogen and stress activated protein kinase-1; MST2, mammalian STE20-like protein kinase; PAK, p21 protein (cdc42/Rac)-activated protein kinase; PDK1, 3-phosphoinositide-dependent protein kinase-1; PHK, phosphorylase kinase; PI3K, phosphoinositide 3-kinase; PIM, proto-oncogene serine-threonine protein kinase; PKA, protein kinase A; PKB/Akt, protein kinase B; PKC, protein kinase C; PKD1, protein kinase D1; PLK, polo-like kinase; PRAK, p38-regulated/activated protein kinase; PRK2, PKC-related kinase-2; ROCK, ρ-dependent protein kinase; RSK, p90 ribosomal S6 kinase; S6K, p70 ribosomal S6 kinase; SGK, serum- and glucocorticoid-induced kinase-1; SmMLCK, smooth-muscle light chain kinase; Src, proto-oncogene tyrosine kinase; SRPK1, serine/arginine protein kinase 1; SYK, spleen tyrosine kinase; TBK1, NF-κ-B-activating kinase; VEG-FR, vascular endothelial growth factor receptor; YES, proto-oncogene tyrosine protein kinase.

 Published on Web 07/10/2009 © 2009 American Chemical Society

Table 1. Activity Profile of **1** and **2** at a Concentration of 10 μM in a Panel of 78 Protein Kinases Presented as Percentage of Kinase Activity Relative to Control Assays without Compound[a]

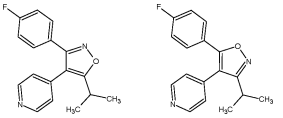

1 **2**

	1	2		1	2
MKK1	76 ± 6	88 ± 12	PLK1	104 ± 5	93 ± 10
ERK1	92 ± 8	87 ± 7	PLK1 (OA)	104 ± 9	105 ± 10
ERK2	86 ± 1	88 ± 1	AURORA B	101 ± 7	22 ± 2
JNK1	67 ± 1	98 ± 0	AURORA C	110 ± 6	35 ± 3
JNK2	13 ± 1	59 ± 6	AMPK	88 ± 8	73 ± 6
JNK3	28 ± 0	63 ± 2	MARK3	95 ± 1	92 ± 2
p38α MAPK	20 ± 6	50 ± 4	BRSK2	87 ± 4	93 ± 7
p38β MAPK	95 ± 13	98 ± 7	MELK	78 ± 3	108 ± 10
p38γ MAPK	84 ± 0	94 ± 9	CK1δ	6 ± 2	55 ± 8
p38δ MAPK	86 ± 6	95 ± 3	CK2	96 ± 10	95 ± 3
ERK8	84 ± 6	88 ± 6	DYRK1A	100 ± 10	95 ± 8
RSK1	79 ± 2	83 ± 3	DYRK2	101 ± 4	104 ± 3
RSK2	113 ± 4	120 ± 2	DYRK3	97 ± 5	101 ± 5
PDK1	82 ± 5	85 ± 9	NEK2a	98 ± 7	96 ± 8
PKBα	94 ± 7	94 ± 9	NEK6	112 ± 12	108 ± 13
PKBβ	101 ± 4	104 ± 6	NEK7	104 ± 7	100 ± 1
SGK1	76 ± 2	91 ± 3	IKKb	103 ± 0	103 ± 8
S6K1	89 ± 2	98 ± 0	PIM1	100 ± 4	89 ± 2
PKA	28 ± 2	90 ± 4	PIM2	105 ± 8	96 ± 1
ROCK 2	76 ± 6	77 ± 3	PIM3	81 ± 4	78 ± 5
PRK2	88 ± 2	98 ± 10	SRPK1	81 ± 7	86 ± 8
PKCα	95 ± 7	104 ± 10	MST2	95 ± 2	95 ± 2
PKCζ	81 ± 15	91 ± 4	EF2K	107 ± 1	107 ± 4
PKD1	60 ± 1	89 ± 8	HIPK2	103 ± 0	103 ± 6
MSK1	95 ± 12	113 ± 2	HIPK3	92 ± 4	100 ± 5
MNK1	96 ± 5	89 ± 4	PAK4	106 ± 12	107 ± 11
MNK2	110 ± 5	101 ± 7	PAK5	98 ± 6	94 ± 7
MAPKAP-K2	105 ± 3	100 ± 8	PAK6	100 ± 1	102 ± 3
MAPKAP-K3	104 ± 9	113 ± 5	Src	72 ± 4	90 ± 1
PRAK	88 ± 3	98 ± 11	Lck	42 ± 0	64 ± 1
CAMKKa	91 ± 6	103 ± 9	CSK	87 ± 13	95 ± 1
CAMKKb	99 ± 5	97 ± 3	FGF-R1	81 ± 10	95 ± 10
CAMK1	75 ± 8	76 ± 9	IRR	93 ± 3	94 ± 4
SmMLCK	99 ± 7	110 ± 1	EPH A2	79 ± 5	81 ± 14
PHK	96 ± 11	99 ± 2	MST4	88 ± 9	102 ± 1
CHK1	91 ± 6	102 ± 6	SYK	131 ± 1	114 ± 8
CHK2	104 ± 0	109 ± 2	YES1	82 ± 7	101 ± 2
GSK3b	75 ± 0	85 ± 8	IKKe	81 ± 2	71 ± 10
CDK2-cyclin A	96 ± 0	98 ± 8	TBK1	90 ± 1	80 ± 6

[a] Results are means ± SD of triplicates. OA: okadaic acid, further abbreviations of protein kinases are given in the list.

in investigating molecular similarities of p38α/CK1δ and in the question if **1** (and related compounds) could serve as lead for the development of potent and selective CK1 inhibitors.

Biological Roles of CK1 and Inhibitors. Protein kinase CK1 represents a highly conserved Ser/Thr protein kinase family, which is ubiquitously expressed in all eukaryotic organisms. The seven mammalian isoforms CK1 α, β, γ1, γ2, γ3, δ, and ε (with various splice variants) are all highly conserved within their kinase domains (~290 residues) but differ significantly within their regulatory short N-terminal and variable C-terminal (ranging in size from 40−180 residues) domains.[13] CK1 becomes constitutively activated due to priming phosphorylation by another kinase such as GSK3β.[14] CK1 can be regulated by inhibitory autophosphorylation, cleavage of the C-terminal domain, and subcellular localization.[15] Physiologically, CK1 isoforms are involved in the regulation of many different cellular processes such as canonical Wnt signaling, DNA damage response, and cell cycle progression.[13,16] Regarding the fact that overstimulation of CK1 isoforms has been linked to the incidence of various types of disorders such as cancer (CK1α/δ/ε),[17] neurodegenerative diseases (CK1δ),[18] and inflammation,[19] the use of CK1 (isoform)-specific inhibitors may have therapeutic potential in the cure of these diseases.[20] Moreover, potent, (isoform)-specific and cell membrane permeable CK1 inhibitors would be useful reagents to further investigate the complex biological roles of this protein kinase family. Despite the actual need, only a few CK1-specific small molecule inhibitors have been described so far

Scheme 1. Synthesis of Isoxazole Derivatives **6**−**10**[a]

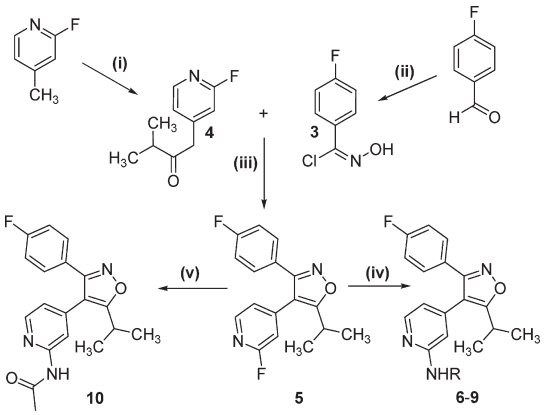

[a] (i) (a) LDA/THF, −78 °C, 1 h; (b) isobutyraldeyde, 3 h; (c) Jones oxidation $K_2Cr_2O_7$/acetone, 0 °C, 2 h. (ii) (a) Hydroxylamine HCl/ethanol, 50%NaOH, rt, 2 h; (b) NCS/DMF, rt, 2 h. (iii) Triethylamine/ethanol, 0 °C, 2 h. (iv) RNH_2, autoclave, 160 °C, 16 h. (v) Pd_2dba_3, Xantphos, CS_2CO_3, CH_3CONH_2, dioxane, reflux.

(Table 2). These include agents such as **21**,[9] **22**,[10] and the more potent and relatively CK1δ-specific compound **23**, which has been recommended for use in cell-based assays.[6] Interestingly, **23** is actually chemically related to the compounds described in this study and has been reported to also inhibit p38α MAPK (62% at a concentration of 10 μM).

Molecular Modeling. To study a rationale for **1** being a potent dual p38α MAPK/CK1δ inhibitor, we compared the molecular architecture of their ATP binding pockets, respectively. In fact, the highly conserved ATP binding sites of p38α and CK1δ (Homologue) revealed a significant structural difference in the gatekeeper position (Figure 1A). Consistent with the in vitro assay data, modeling studies for **1** demonstrated reasonable binding modes in the ATP pocket of both p38α and CK1δ (Figure 1B). In an analogous manner to ATP binding, the pyridine ring nitrogen is accepting a hydrogen bond from the backbone NH/Met109 (p38α) and NH/Leu88 (CK1δ), respectively. The 4-fluor-phenyl moiety is situated in the hydrophobic pocket I (HPI, "selectivity pocket") lined by gatekeeper residue Thr106 (p38α) and Met85 (CK1δ), which are embraced by the vicinal aromatic systems of the inhibitor, respectively.

Concerning an optimization strategy for lead **1**, the rational binding modes suggested a second vicinal H-bond interaction to the carbonyl oxygen of Met109/p38α and Leu88/CK1δ in the hinge region (binding mode exemplified for compound **10**, see Figure 1C). Accordingly to this concept, we hypothesized that such an interaction could be achieved by introducing an NH moiety suitable as H-bond donor at the 2′ position of pyridine in **1**.[21] To prove this hypothesis, we synthesized a small variety of amines (**6**−**9**) and amides (**10**−**13**) and evaluated their SAR toward p38α and CK1δ.

Chemistry. To investigate SAR for the NH-substituted 2′-pyridine position of lead **1**, a flexible and straightforward synthesis toward 2′-aminopyridin-4-yl/4-fluorophenyl-isoxazoles was developed (Scheme 1). Key intermediate **5** was prepared in high yield by our established method for the synthesis of 3,4-diarylisoxazoles by 1,3-cycloaddition.[2] Subsequent substitution of the 2-fluoro-pyridine moiety by secondary amines was achieved by conventional amination at 160 °C under high pressure in an autoclave.[26] This reaction

Table 2. Selected Compounds Reported to Have Potency against CK1δ and p38α MAPK (nd*: To the Best of Our Knowledge, No Data Has Been Published)

#	structure	inhibition CK1δ	inhibition p38α
19 (SB203580)	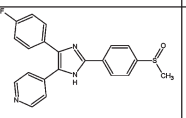	92 ± 1 % at 1 μM[6]	IC_{50} = 0.04 μM[8]
20 (SB202190)	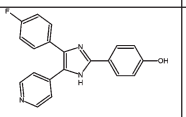	79 ± 1% at 1 μM[6]	IC_{50} = 0.05 μM[8]
21 (IC261)	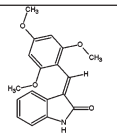	IC_{50} = 1 μM[9]	no inhibition at 25 μM[6]
22 (CKI-7)	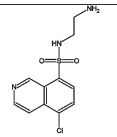	IC_{50} = 10 μM[10] (88 ± 1 % at 25 μM)[6]	no inhibition at 25 μM[6]
23 (D4476)	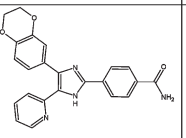	IC_{50} = 0.3 μM[11]	IC_{50} = 12 μM[11]
24 (1,4-diaminoanthra-9,10-quinone)	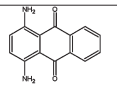	IC_{50} = 0.33 μM[12]	nd*

proceeds as a nucleophilic aromatic substitution (S_N-Ar/addition−elimination mechanism) and yielded derivatives **6**−**9**. (X-ray analysis for **7**, **8**, and **9** is available in Supporting Information). In contrast, substitution of the 2-fluoro-pyridine moiety in **5** by amides turned out to be more difficult. Initially, a strategy involving a modified Hartwig−Buchwald[27] reaction was employed for the preparation of **10** (Scheme 1).

This reaction involved cross-coupling of **5** and 3 equiv of acetamide in the presence of 2 mol % of Pd_2dba_3, 6 mol % Xantphos, and 1.4 equiv of Cs_2CO_3 in anhydrous dioxane under reflux. However, under these reaction conditions, the yield of **10** was not satisfying (15%) and the purification process was rather tedious. All attempts to increase the yield by varying reaction conditions such as using other ligands, bases, longer reaction time (> 24 h), and higher temperature (toluene, reflux) were unsuccessful. A major reason could be the low reactivity of 2-fluoropyridine **5** in this reaction whereby the strong fluorine−carbon bond disfavors the oxidative insertion of the palladium catalyst. Accordingly, we established a more convenient approach for the synthesis of further amides by using the intermediate 2-aminopyridyl **12** as suitable precursor (Scheme 2).

An effective procedure for the preparation of 2-aminopyridine **12** proved to be the reaction of 2-fluoropyridine derivative **5** with sodium azide[28] to yield the corresponding tetrazolo derivative **11**, which was reduced to **12** by several techniques (Scheme 2). Two reduction methods were investigated for the preparation of **12** from **11**: tin(II)chloride dihydrate[29] in methanol at 50 °C and catalytic hydrogenation performed at low hydrogen pressure with 10% Pd/C.

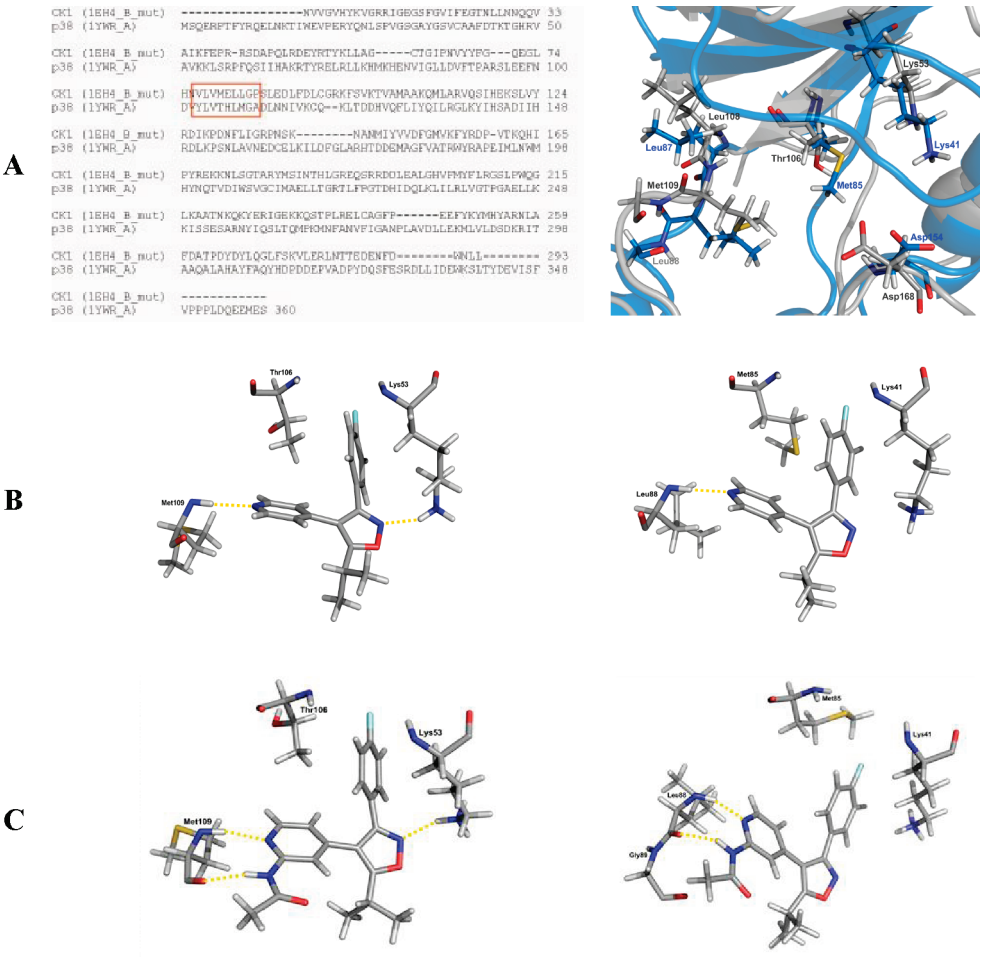

Figure 1. (A, left) Sequence alignment of CK1δ Homologue (PDB code 1EH4[9]), and p38α (PDB code 1YWR[22]) with highlighted residues of the hinge region; (right) Overlay of ATP binding pocket of p38α (PDB 1A9U,[23] gray) and CK1δ (PDB 1CKI,[24] blue). Binding modes of **1** (B) and **10** (C) in the ATP binding pocket of p38α (left) and CK1δ (right). Key residues and H-bond interactions to the hinge region (Met109/p38α; Leu88/CK1δ) are shown. The vicinal pyridin-4-yl/4-F-phenyl moieties clasping around the gatekeeper residue (Thr106/p38α; Met85/CK1δ) positioning the 4-F-phenyl in HPI ("selectivity pocket").[3] In the pose of **1** and **10** in p38α the isoxazole ring nitrogen is accepting an H-bond from conserved but flexible Lys53.[25] However, a comparable interaction was not calculated for Lys41 in CK1δ although this residue is situated in a similar position.

Scheme 2. Synthesis of Building Block **12** from **5** via Tetrazole **11**[a]

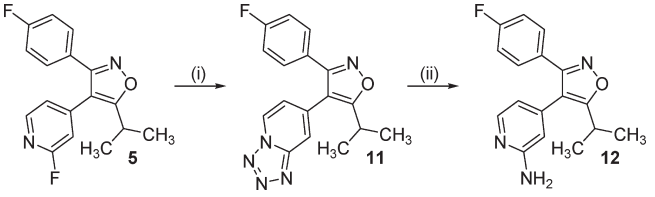

[a] Reagents: (i) sodium azide, DMSO, 140 °C, 3 h. (ii) Reduction method (A) tin(II)chloride dihydrate, MeOH, 50 °C, 3 h; or method (B) autoclave H_2 (5 bar), 10% Pd/C, MeOH, catalytic amount of HCl, room temperature, 24 h.

Although the latter method proceeded in a cleaner reaction, the yield obtained from the former technique was higher. Having **12** in hand, we next investigated methods for the substitution of the aminopyridine moiety. The synthesis of **13** was successfully carried out by reacting **12** with freshly prepared 2-(4-fluorophenyl)acyl chloride and triethylamine in toluene under reflux. Accordingly, **14** was prepared by using commercially available 2-phenoxypropanoylchloride and 4-(dimethylamino)pyridine in toluene at 60 °C. The coupling reagent *N*,*N*′-carbonylimidazole (CDI) was utilized to activate (*E*)-(2,4-dimethoxyphenyl)-cinnamic acid for the final step for the preparation of **15**. Taken together, intermediate **12** can be used as a building block to generate 2-amido substituted pyridine derivatives.

Biological Evaluation and Discussion

Compounds **6**−**10** and **13**−**15** were initially screened for their biological activity in a p38α (IC_{50})[8] assay and CK1δkd (kinase domain)[30] assay at a concentration of 10 μM. Agents showing significant inhibition of CK1δkd were further characterized for their IC_{50} value against CK1δkd and GST-CK1δ (GST-rat CK1δ fusion protein full length;[31] results are presented in Table 3). While the unsubstituted lead **1** (3-(4-fluorophenyl)-5-isopropylisoxazol-4-yl-pyridine) actually proved to be a submicromolar dual inhibitor of these kinases (IC_{50} p38α = 0.45 μM, IC_{50} GST-CK1δ = 0.23 μM), the 2′- pyridine-butylamine derivative **6** was determined with an IC_{50} value of 0.03 μM against p38α but single digit μM-activity against CK1δkd. Similar results were obtained for **7** (*N*-tetrahydro-2*H*-pyran-4-ylpyridin-2-amine) as well as for enantioselective synthesized *N*-(1*R*/*S*-1-phenylethyl)pyridin-2-amines **8** and **9** (structures proven by X-ray analysis, see

Table 3. Isoxazole Derivatives **6**−**10** and **13**−**15** and Their Biological Activity against p38α, CK1δkd (Kinase Domain[a]) and GST-CK1δ (GST-ratCK1δ[b])[c]

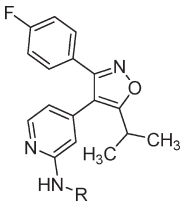

#	R	IC_{50} (μM) p38α[g]	IC_{50} (μM) CK1δkd[a]	IC_{50} (μM) GST-CK1δ[b]
6		0.03 ± 0.01	-	-
7		0.06 ± 0.02	2.5 ± 0.12	-
8 (*R*)		0.45 ± 0.11	-	-
9 (*S*)		0.006 ± 0	1.6 ± 0.52	-
10		0.30 ± 0.19	0.7 ± 0.15	0.33 ± 0.1
13		1.56 ± 0.78	0.11 ± 0.04	0.09 ± 0.03
14 (*rac R,S*)		0.89 ± 0.08	0.82 ± 0.25	0.34 ± 0.16
15		2.52 ± 0.48	0.033 ± 0.01	0.047 ± 0.03

[a] Isoxazole derivatives **6**−**10** and **13**−**15** and their biological activity against p38α, CK1δkd (kinase domain). [b] Isoxazole derivatives **6**−**10** and **13**−**15** and their biological activity against GST-CK1δ (GST-ratCK1δ). [c] Results are presented as mean ± SD from experiments performed at least in duplicate.

Supporting Information), the latter *S*-enantiomer having excellent potency against p38α (IC_{50} = 0.006 μM) with strong selectivity over CK1δ (IC_{50} CK1δkd = 1.6 μM, ratio IC_{50} p38α/CK1δkd = 0.0038).

In contrast, the amides **10**, **13**, **14**, and **15** showed dual activity against p38α and CK1δ. In detail, *N*-acetamide **10** and racemic *N*-2-phenoxypropanamide **14** were determined to have comparable potency against p38α MAPK and CK1δ. These results were in line with the binding mode of **10** in both kinases (Figure 1C). Because **14** was prepared and assayed as a racemic mixture, no inhibition data for the defined enantiomers can be revealed. However, notable selectivity for CK1δ was observed for *N*-(2-(4-fluorophenyl)acetamide **13** (ratio IC_{50} CK1δkd/p38α = 0.07). Moreover, (*E*)-3-(2,4-dimethoxyphenyl)-*N*-acrylamide derivative **15** was determined to be the most potent and selective CK1δ inhibitor in this series (IC_{50} CK1δkd = 0.033 μM, IC_{50} p38α = 2.52 μM; ratio IC_{50} CK1δkd/p38α = 0.013).

To investigate the partial selectivity of amine **9** for p38α and of amide **15** for CK1δ, we compared their modeled binding modes in these kinases, respectively (Figure 2). Consistent with the pose of lead **1** (Figure 1B) and according to the design idea of pyridine 2′ substitution (Figure 1C), similar plausible binding modes for **9** and **15** in the ATP binding pockets of p38α and CK1δ were calculated (Figure 2). These involve central bidentate H-bond interactions of the pyridine-nitrogen/2′-NH-moiety to the hinge region (Met109/p38α; Leu88/CK1δ, not shown for clarity). The 4-F-phenyl is situated in the "selectivity pocket" (HPI), whereas the pyridine 2′-substituted moiety is accommodated by the hydrophobic region II (HRII) toward the solvent accessible part of the ATP binding site. In particular, the *S*-1-phenylethylpyridine side chain moiety in **9** addresses a lipophilic cleft in HRII of p38α (surrounded by Gly110/Ala111/Asp112/Ala157). This pose is consistent with the stereochemically defined *S*-orientation of **9**, and a comparable binding mode was not found for its *R*-enantiomer **8**. In contrast to the situation in p38α, the less spacious and planar HRII of CK1δ is forcing a tilted conformation of **9**, resulting in poorer overall geometry of binding interactions. However, these binding modes were in line with biological data and may explain the excellent potency and partial selectivity of **9** for p38α over CK1δ.

On the other hand, the binding modes of **15** in p38α and CK1δ, respectively, revealed further differences in HRII, which may account for the potency and relative selectivity of **13** for CK1δ over p38α. Most importantly, the elongated planar (*E*)-3-(2,4-dimethoxyphenyl)-*N*-acrylamide moiety in **15** is faintly situated in HRII of p38α, actually reaching well into the solvent space. By contrast, in CK1δ the 2,4-dimethoxyphenyl moiety is accommodated by Pro142/Arg141/Glu37/Leu87 belonging to an extended loop (termed L7/8 loop)[32] that is not present in p38α (Figure 3). Again, the binding modes described above go parallel with the in vitro assay data and therefore could explain the partial selectivity of **15** for CK1δ over p38α.

Given this reasonable binding modes, it is noteworthy that in principle the acrylamide moiety in **15** could function as a Michael acceptor addressing a chemically reactive amino acid residue (such as cysteine), thereby forming a covalent bond to the protein. However, a cysteine residue capable of reacting through this mechanism cannot be found either in HRII of p38α or in HRII of CK1δ. Moreover, related agents **17** and **18** were shown to be ATP dependent inhibitors of CK1δ (Figure 5, for details and discussion see below), providing further evidence against the Michael reactivity.

Scaffold Hopping: From Isoxazoles to Imidazoles. Motivated by the CK1δ-selective isoxazole-based inhibitor **15**, we wondered if the concept involving the (*E*)-3-(2,4-dimethoxyphenyl)-*N*-acrylamide moiety could be applied to an imidazole scaffold that is present in prototypical p38α inhibitors.[4] To address this question, we reacted 4-[5-(4-fluoro-phenyl)-2-methylsulfanyl-3*H*-imidazol-4-yl]-pyridin-2-ylamine (**16**)[33] with activated 2,4-dimethoxycinnamic acid (CDI method) to yield compound **17**. Subsequent sulfoxidation using potassium peroxomonosulfate (Oxone) as an oxidating agent gave compound **18** (Scheme 3).

Biological Characterization of Compounds 17 and 18 (CKP138). Compounds **17** and **18** were tested for their potency against p38α and the GST-CK1δ fusion protein (Table 4). Fortunately, these compounds could be identified to be extremely effective in blocking GST-CK1δ kinase activity (**17** IC_{50} = 0.00448 μM; **18** IC_{50} = 0.01077 μM) and thus are among the most potent inhibitors for CK1δ known so far (see Table 2). However, low nM IC_{50} values against p38α were also found (**17** IC_{50} = 0.019 μM; **18** IC_{50} = 0.041 μM). To assess CK1 isoform specificity, these two inhibitors were additionally tested for their ability to inhibit CK1ε, which is exhibiting the highest relation to CK1δ among the CK1 isoforms. Interestingly, IC_{50} values determined for CK1ε are reduced by 15-fold for **17** and even

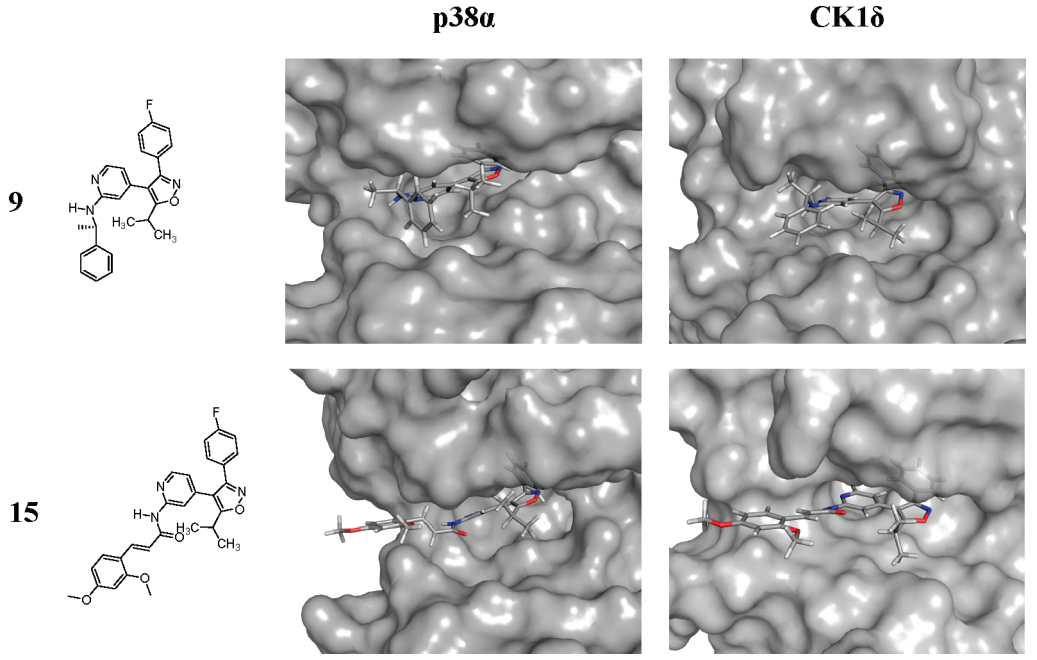

Figure 2. Comparison of modeled binding modes of **9** and **15** in the ATP binding pocket of p38α MAPK (PDB code 1YWR)[22] and CK1δ Homologue (PDB code 1EH4),[9] respectively. The proteins are presented with their Connolly surface (colored in gray) to illustrate more clearly structural differences especially in the solvent accessible part of HRII.

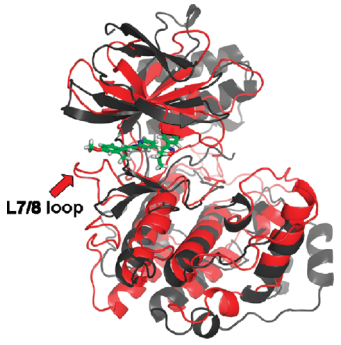

Figure 3. Structure alignment of p38α MAPK (illustrated in black, PDB code 1YWR)[22] and CK1δ Homologue (illustrated in red, PDB code 1EH4)[9] with modeled binding mode of **15** (highlighted in green) in the ATP binding pocket of CK1δ. Herein, the 2,4-dimethoxyphenyl moiety of **15** interacts with a loop (termed L7/8 loop)[32] not present in p38α.

41-fold for **18** (Figure 4) compared to those determined for CK1δ. These results impressively demonstrate that in low concentrations near the determined CK1δ IC_{50} values, compounds **17** and especially **18** preferentially inhibit CK1δ.

Compounds 17 and 18 are ATP Competitive Inhibitors of CK1δ. To prove these compounds as ATP competitive inhibitors, **17** and **18** were tested at a concentration matching the IC_{50} value for their potency to inhibit CK1δ in the presence of varying amounts of ATP (Figure 5). This experiment revealed that the IC_{50} values increased progressively as the concentration of ATP escalated, thus confirming the ATP competitive properties of **17** and **18**. However, even in presence of highest ATP concentration (500 μM), the compounds still show an inhibition of kinase activity by 18% (**17**) and 10% (**18**).

Regarding a possible irreversible binding mode of **17** and **18** bearing the acrylamide moiety (Michael reactivity as discussed above), one would expect the compounds to

Scheme 3. Synthesis of 2-Acylaminopyridine-4-yl-imidazole Derivatives **17** and **18**[a]

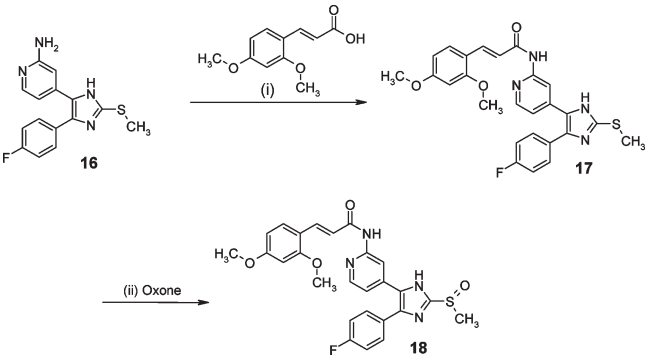

[a] (i) CDI, 2,4-dimethoxycinnamic acid, dioxane, room temperature. (ii) THF, water, potassium peroxomonosulfate (Oxone reagent).

block CK1δ activity independent from ATP concentrations in the assay. However, this experiment provided evidence that the acrylamide moiety in **17** and **18** is not covalently linking the compounds to the protein.

Compounds 17 and 18 Show No Significant Inhibition of a CK1δ-Gatekeeper Mutant. In line with the binding modes of isoxazoles (Figure 2), a comparable pose was determined for **18** in CK1δ (Figure 6, left). As discussed above, in this model, amino acid 85 (methionine) takes the central role of gatekeeper residue, which is embraced by the aromatic systems of this compound thereby controlling access of the 4-F-phenyl moiety to the "selectivity pocket". To verify the gatekeeping property of methionine a GST-CK1δ^{M82F} mutant (corresponding to position 85 in the docking model) was generated by site directed mutagenesis. Instead of methionine, the mutant (referred to as GST-CK1δ^{M82F}) carries the more bulky amino acid phenylalanine and therefore was expected to prevent access of the compounds to the ATP binding pocket while still binding ATP (cofactor ATP in

Table 4. Imidazole Derivatives **17** and **18** and Their Biological Activity against p38α,[8] CK1δkd (Kinase Domain), GST-CK1δ (GST-ratCK1δ Fusion Protein), and CK1ε (Full Length Protein[31])[a]

no.	IC_{50} (μM) p38α	IC_{50} (μM) CK1δkd[b]	IC_{50} (μM) GST-CK1δ[c]	IC_{50} (μM) CK1ε[d]
17	0.019	0.004 ± 0	0.005 ± 0	0.073 ± 0.01
18	0.041	0.005 ± 0	0.011 ± 0.03	0.447 ± 0.08

[a] Results are presented as mean ± SD from experiments performed at least in duplicate. [b] Imidazole derivatives **17** and **18** and their biological activity against p38α, CK1δkd[8] (kinase domain). [c] Imidazole derivatives **17** and **18** and their biological activity against GST-CK1δ (GST-ratCK1δ fusion protein). [d] Imidazole derivatives **17** and **18** and their biological activity against CK1ε (full length protein).

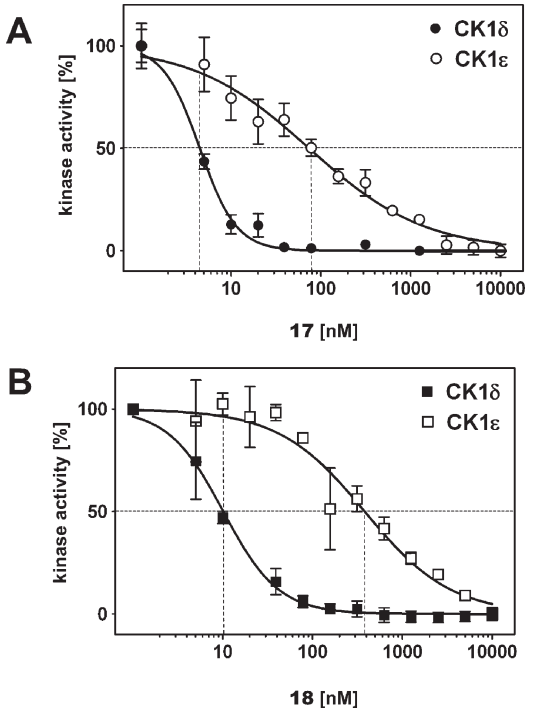

Figure 4. Determination of CK1 isoform specificity. Compounds **17** (A) and **18** (B) exhibit different effects on GST-CK1δ (filled circles/squares) and CK1ε (open circles/squares). Both compounds more potently inhibit CK1δ, showing specificity toward this isoform in concentrations around the IC_{50}'s determined for GST-CK1δ.

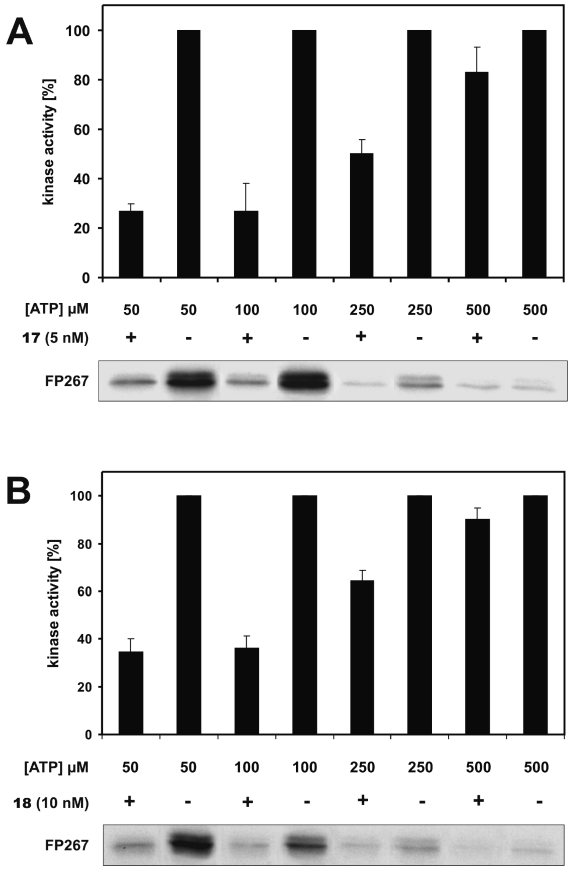

Figure 5. Compounds **17** and **18** inhibit CK1δ in an ATP competitive manner. Inhibitors **17** (5 nM) (A) and **18** (10 nM) (B) were assayed on CK1δkd in the presence of the indicated ATP concentrations. Kinase assays were perfomed using CK1δkd as enzyme and GST-$p53^{1-64}$ fusion protein (FP267) as substrate. Kinase activity in reactions containing inhibitor was calculated relative to the control reaction for each ATP concentration ($n = 3 \pm$ SD). While ATP concentrations increase, incorporation of radioactive labeled phosphate into GST-$p53^{1-64}$ fusion protein FP267 decreases, leading to weakened signals in the autoradiographs.

general is not occupying the selectivity pocket in kinases). In vitro kinase assays were performed in the absence and presence of **17** and **18** at concentrations of 5 and 10 nM, respectively, using GST-CK1δ or GST-$CK1\delta^{M82F}$ as a source of enzyme. As expected, GST-CK1δ kinase activity was clearly decreased in the presence of **17** (5 nM) and **18** (10 nM). In contrast, kinase activity of GST-$CK1\delta^{M82F}$ was not affected in reactions containing 5 nM **17** or 10 nM **18**, respectively (Figure 6, right), thus strongly supporting the modeled binding mode. However, kinase activity of GST-$CK1\delta^{M82F}$ was increased in control reactions by 42% compared to GST-CK1δ wild-type controls, suggesting a stronger ATP turnover rate for the mutant. The increase in kinase activity detected for GST-$CK1\delta^{M82F}$ may result from conformational alterations occurring in the mutant, which may lead to a more effective binding of ATP or substrate leading to enhanced incorporation of phosphate into the substrate.

Selectivity Profiling of Compounds 17 and 18 in a Panel of 76 Protein Kinases. To investigate the specificity of these compounds, we studied their effect at concentrations of 0.1 μM in a panel of 76 protein kinases (Table 5, further details available in Supporting Information). The assays used ATP concentrations for each kinase which approximate the K_m constant for ATP.[6] In this panel, CK1δ and p38α were potently inhibited by **17** and **18**, while most of the kinases were not affected significantly. However, at 0.1 μM, both compounds blocked very few kinases to a similar extent (**17**: p38β by 83%, JNK2 by 69%, MKK1 by 73% and YES1 by 76%; **18**: p38β by 54%, JNK2 by 88%, MKK1 by 82%, and YES1 by 86%). Importantly, in this panel, kinases involved in regulation of CK1 such as GSK3β, PKC, PKA, and CHK1 were not blocked, suggesting **18** could be a suitable pharmacological tool to further investigate the biological roles of CK1δ in cells.

Cellular Efficacy of Compounds: Inhibition of Growth of the Human Extravillous Trophoblast Hybrid Cells AC1-M88. Although potent inhibition of CK1δ could be shown for a variety of compounds against the isolated enzyme, they might not necessarily act the same way in cellular

experiments. To identify inhibitors that are able to pass cell membranes and to show efficacy in more physiological conditions, compounds were tested using the human immortal, invasive extravillous trophoblast hybrid cell line (AC1-M88) using apoptosis for readout as described previously.[34]

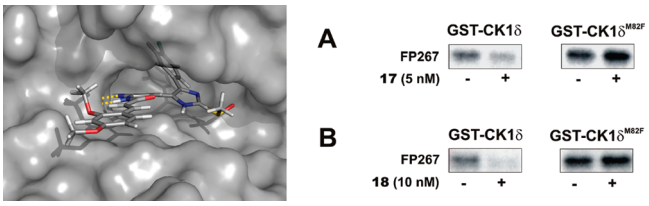

Figure 6. (left) Modeled binding mode of **18** in the ATP binding pocket of CK1δ Homologue (PDB code 1EH4[9]) to illustrate the role of gatekeeper (center) controlling access of the 4-F-phenyl moiety to the "selectivity pocket" (background). (right) Inhibition of CK1δ wild-type and a M82F gatekeeper mutant by **17** and **18** as judged by autoradiographs using GST-p53$^{1-64}$ fusion protein (FP267) as substrate. While GST-CK1δ wild-type activity shows clear reduction by **17** (A) and **18** (B), the gatekeeper mutant GST-CK1δ^{M82F} is barely influenced under the same conditions. As indicated in the autoradiographs, the activity of GST-CK1δ^{M82F} was approximately 42% higher compared to GST-CK1δ wild-type.

Because of the heterogeneous expression of a p53 polymorphism, AC1-M88 cells generally show a higher apoptosis rate upon treatment with the CK1-specific inhibitor **21** (IC261) than the wild-type p53 expressing CV-1 cells.[34] On the basis of preliminary experiments (data not shown), in this study AC1-M88 cells were treated with compounds **15**, **17**, and **18** using a 50-fold concentration of their respective IC_{50} values. Namely AC1-M88 cells were incubated with **15** (3.32 μM), **17** (0.38 μM), **18** (0.26 μM), or CK1 inhibitor **21** (IC261, 8 μM)[9] for 48 h, fixed and stained with propidium iodide for flow cytometrical analysis. Treatment of AC1-M88 cells with **21** (8 μM) as positive control[9] led to a high amount of dead cells after 48 h (84.0%; Figure 7). Interestingly, application of test compounds also resulted in cell death to a similar extend. After 48 h, almost all cells either treated with **17** (87.1%), or **18** (77.1%) were dead, whereas less amount of dead cells (34.4%) were observed upon treatment with **15**. In contrast, cells applied with solvent alone (negative control, final assay concentration 0.004% DMSO) had no effect on cell cycle progression. These results correlate with the data from CK1δ enzyme assays and clearly indicate cell permeant inhibitors **17** and **18** to be highly effective in AC1-M88 cells at submicromolar concentrations.

Table 5. Activity Profile of **17** and **18** at a Concentration of 0.1 μM in a Panel of 76 PK Presented as % Mean Residual Activity to Control Assays without Compound ($n = 3 \pm$ SD)[a]

	17	**18**		**17**	**18**
MKK1	27 ± 10	18 ± 15	AMPK	92 ± 0	99 ± 1
ERK1	94 ± 10	101 ± 5	MARK3	87 ± 2	89 ± 0
ERK2	91 ± 8	93 ± 8	BRSK2	86 ± 1	97 ± 3
JNK1	90 ± 1	53 ± 2	MELK	81 ± 5	92 ± 5
JNK2	31 ± 2	12 ± 0	CK1	10 ± 1	18 ± 2
p38a MAPK	3 ± 4	5 ± 4	CK2	115 ± 8	122 ± 6
P38b MAPK	17 ± 3	46 ± 2	DYRK1A	78 ± 7	86 ± 5
p38g MAPK	84 ± 17	97 ± 15	DYRK2	82 ± 10	101 ± 13
p38d MAPK	90 ± 5	100 ± 5	DYRK3	104 ± 3	90 ± 1
ERK8	83 ± 0	88 ± 0	NEK2a	91 ± 4	92 ± 8
RSK1	78 ± 6	80 ± 8	NEK6	90 ± 5	111 ± 17
RSK2	86 ± 7	94 ± 14	IKKb	84 ± 11	87 ± 2
PDK1	74 ± 6	94 ± 8	PIM1	98 ± 4	109 ± 0
PKBa	105 ± 1	105 ± 7	PIM2	87 ± 22	101 ± 5
PKBb	98 ± 0	100 ± 28	PIM3	81 ± 2	90 ± 8
SGK1	87 ± 7	87 ± 4	SRPK1	91 ± 8	97 ± 7
S6K1	67 ± 4	74 ± 0	MST2	97 ± 2	112 ± 5
PKA	84 ± 7	92 ± 5	EF2K	100 ± 2	102 ± 8
ROCK 2	81 ± 6	88 ± 6	HIPK2	94 ± 2	104 ± 4
PRK2	95 ± 7	96 ± 2	PAK4	81 ± 8	98 ± 1
PKCα	110 ± 2	103 ± 15	PAK5	94 ± 3	105 ± 7
PKCζ	79 ± 13	83 ± 8	PAK6	76 ± 2	84 ± 3
PKD1	88 ± 13	97 ± 3	Src	49 ± 2	63 ± 5
MSK1	84 ± 2	97 ± 3	Lck	50 ± 9	74 ± 7
MNK1	91 ± 9	96 ± 1	CSK	81 ± 4	79 ± 2
MNK2	85 ± 11	88 ± 1	FGF-R1	50 ± 0	50 ± 14
MAPKAP-K2	82 ± 7	78 ± 6	IRR	61 ± 1	83 ± 1
PRAK	83 ± 4	101 ± 6	EPH A2	97 ± 5	95 ± 21
CAMKKb	88 ± 2	92 ± 9	MST4	90 ± 7	86 ± 3
CAMK1	92 ± 13	98 ± 7	SYK	86 ± 1	86 ± 9
SmMLCK	82 ± 7	93 ± 6	YES1	24 ± 4	14 ± 1
PHK	99 ± 8	102 ± 3	IGF-1R	87 ± 1	107 ± 7
CHK1	80 ± 6	88 ± 4	VEG-FR	33 ± 0	46 ± 3
CHK2	79 ± 2	85 ± 3	BTK	92 ± 2	105 ± 5
GSK3b	81 ± 4	101 ± 12	IR-HIS	94 ± 8	94 ± 9
CDK2-cyclin A	112 ± 16	115 ± 4	EPH-B3	94 ± 7	95 ± 17
PLK1	97 ± 3	110 ± 2	TBK1	103 ± 7	106 ± 1
AURORA B	93 ± 10	93 ± 8	IKKe	97 ± 0	90 ± 1

[a] Abbreviations of protein kinases are given in the list, further details of assays are available in Supporting Information.

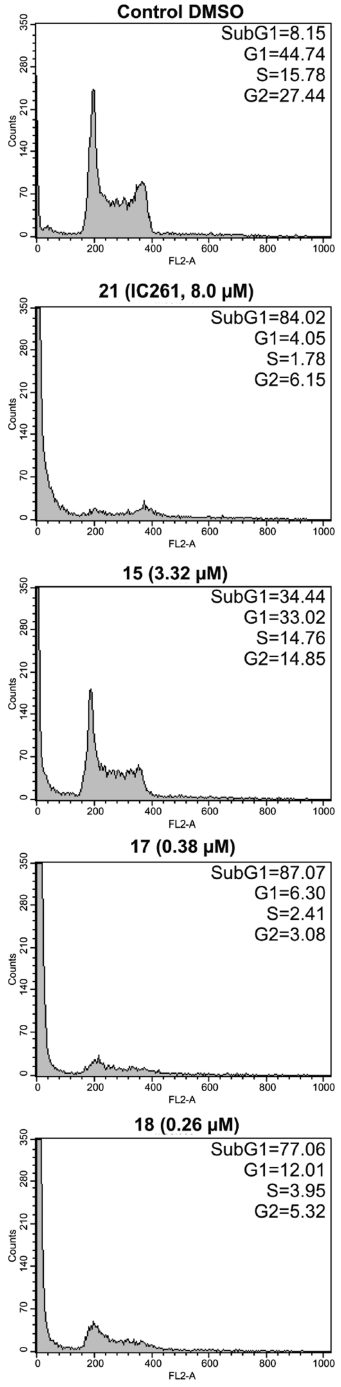

Figure 7. Cell cycle FACS analysis of extravillous trophoblast hybrid (AC1-M88) cells treated with compounds **15**, **17**, **18**, and **21** (IC261). AC1-M88 cells were incubated with compounds **21** (IC261, 8 μM),[9] **15** (3.32 mM), **17** (0.38 mM), or **18** (0.26 mM) for 48 h, stained with propidium iodide, and analyzed in the flow cytometer using a Becton Dickinson "FACScan" flow cytometer. DMSO treated control cells showed a normal cell cycle distribution of asynchronously proliferating cells. Treatment of AC1-M88 cells with **21** (IC261) or compounds **17** and **18** resulted in cell death to a similar extent, whereas **15** was less effective.

Conclusion

Derived from p38α inhibitor **1** as initial lead structure, highly potent ATP competitive dual-specific inhibitors of CK1δ and p38α could be identified, namely **17** (GST-CK1δ $IC_{50} = 0.004\ \mu M$; p38α $IC_{50} = 0.019\ \mu M$) and **18** (GST-CK1δ $IC_{50} = 0.011\ \mu M$; p38α $IC_{50} = 0.041\ \mu M$). With IC_{50} values in the single digit nanomolar range, these inhibitors are among the most potent inhibitors for CK1δ known so far. Assaying inhibitor potency on CK1ε also revealed a strong isoform specificity of **17** and **18** toward CK1δ in low nanomolar concentrations. However, only CK1δ and the closely related CK1ε have been tested so far. Additional experiments are necessary to characterize their effects on the CK1α and γ isoforms and their various splice variants. Testing compounds **17** and **18** in the gatekeeper mutant (GST-CK1δ^{M82F}) assay revealed that kinase activity was not influenced. This result strongly supports the modeled binding mode in the ATP binding pocket of CK1δ. The potent in vitro CK1δ inhibitors **17** and **18** demonstrated cellular efficacy due to their ability to induce apoptotic processes in AC1-M88 cells, a cell line which already has been shown to respond to treatment with **21** (IC261).[34] However, CK1 is involved in a variety of cellular functions and effects of CK1 specific inhibitors are dependent on the cellular background.[34] Therefore, further experiments will be necessary to characterize the impact of these compounds on cellular CK1δ signaling more deeply. Taken together, we recommend compounds **17** and **18** (CKP138) as pharmacological tools to further investigate the exciting roles of CK1δ in signal transduction pathways. Although compounds described in this study can find use for applications unraveling new functional properties of protein kinases, the dissection of cellular effects derived from inhibition of CK1δ and p38α MAPK, respectively, will be crucial. This could be achieved by using the highly potent and selective p38α inhibitor **9** compared to the dual p38α/CK1δ inhibitor **18** (CKP138). Targeting CK1 with specific inhibitors is effective in particular in proliferative diseases and the demand for potent CK1-specific inhibitors has increased over the last years. Therefore, the development of such agents and their screening for in vivo applications will get more in focus in future.

Experimental Section

Chemistry. Infrared spectra were recorded on a "Perkin Elmer Spectrum One" infrared spectrophotometer. ^1H (200 MHz, digital resolution 0.3768 Hz) and ^{13}C (50 MHz, digital resolution 1.1299 Hz) NMR were recorded on a Bruker AC 200. The data are reported as follows: chemical shift in ppm from Me_4Si as external standard, multiplicity and coupling constant (Hz). GC/MS was performed on a HP6890 series system. EI-Mass spectra were recorded on a Varian MAT 311A (70 eV). HRMS and FD-Mass spectra were recorded on a MAT-95 (Finnigan). For clarity, only the highest measured signal is given for FD-mass spectra. Melting points/decomposition temperatures were determined on a Buchi apparatus according to Dr. Tottoli and are uncorrected. X-ray structure determination was performed on a CAD4-Enraf-Nonius using Cu Kα radiation with graphite monochromator. Where appropriate, column chromatography was performed for crude precursors with Merck Silica Gel 60 (0.063−0.200 mm) or Acros organics silica gel (0.060−0.200 mm; pore diameter ca. 60 nm). Column chromatography for test compounds was performed using a La-Flash-System (VWR) with Merck Silica Gel 60 (0.015−0.040 mm) or RP8 columns. The progress of the reactions was monitored by thin-layer chromatography (TLC) performed with Merck Silica Gel 60 F-245 plates. Where necessary, reactions were carried out in a nitrogen atmosphere using 4 Å molecular sieves. All reagents and solvents were obtained from commercial sources and used as received (THF was used after distillation over K/benzophenone). Reagents were purchased from Sigma-Aldrich Chemie, Steinheim, Germany; Lancaster Synthesis, Muhlheim, Germany, or Acros, Nidderau, Germany.

HPLC analysis was performed on a Hewlett-Packard HP 1090 series II using a Thermo Betasil C8 (150 μM × 4.65 μM) column (mobile phase flow 1.5 mL/min, gradient KH_2PO_4 buffer pH 2.3/methanol, UV-detection 230/254 nm). All key compounds were proven by this method to show ≥95% purity. Additionally, HRMS analysis was performed for test compounds. A table summarizing the purity of key target compounds can be found at Supporting Information.

The synthetic procedures for preparation of **1** and its regioisomer **2** were described in our previous work.[2] Experimental and spectroscopic data for nonkey compounds **3**, **4**, and **5** can be found at Supporting Information.

General Procedure for the Preparation of Compounds (6−9). In an autoclave compound, 2-fluor-4-(3-(4-fluorophenyl)-5-isopropyl-4-yl)pyridine (**5**, 1 mmol) was suspended in an excess volume of the respective amine (approx 10 mmol). The mixture was stirred at 160 °C for 24 h. The reaction was cooled to rt. The resulted black residue was washed with water and extracted with CH_2Cl_2. The organic phase was dried over Na_2SO_4 and concentrated in vacuo. The residue was purified by flash chromatography (SiO_2, eluent: petrol ether−ethyl acetate, mixing ratio given for each compound, respectively) to afford the respective compound.

***N*-*sec*-Butyl-4-[3-(4-fluorophenyl)-5-isopropylisoxazol-4-yl]pyridin-2-amine (6).** This compound was obtained according to general procedure from compound **5** (0.2 g, 0.67 mmol) and butan-2-amine (0.5 g, 7 mmol). The residue was purified by flash chromatography (SiO_2, eluent: petrol ether 75%−ethyl acetate 25%) to afford the title compound as white solid. Melting point: 136 °C. ^{1}H NMR ($CDCl_3$, 200 MHz, ppm): δ (ppm) 0.89 (t, J = 7.48 Hz, 3H, *sec*-butylamine), 1.13 (d, J = 6.34 Hz, 3H, *sec*-ba), 1.36 (d, J = 6.95 Hz, 6H, 2 × CH_3), 1.47 (m, 2H, *sec*-butylamine), 3.19 (m, 1H, *sec*-butylamine), 3.49 (m, 1H, *sec*-butylamine), 4.55 (d, J = 7.98 Hz, 1H, NH), 6.07 (s, 1H, 4-Pyr), 6.35 (d, J = 5.13 Hz, 2H, 4-Pyr), 7.03 (m, 2H, 4-F-ph), 7.46 (m, 2H, 4-F-ph), 8.05 (d, J = 4.99 Hz, 1H, 4-Pyr). ^{13}C NMR ($CDCl_3$, 200 MHz, ppm): δ (ppm) 10.2 (CH_3, −2-But-amine), 20.0 (2 × CH_3), 20.9 (CH_3, −2-But-amine), 26.4 ($CHMe_2$), 29.5 (CH_2, −2-But-amine), 48.5 (CH, −2-But-amine), 107.1 (C-5), 112.4 (C-4′), 113.4 (C-3), 115.5 (d, $^2J_{C-F}$ = 21.7 Hz, C-3″/C-5″), 124.8 (d, $^4J_{C-F}$ = 3.3 Hz, C-1″), 130.2 (d, $^3J_{C-F}$ = 8.4 Hz, C-2″/C-6″), 139.9 (C-4), 148.7 (C-6), 158.5 (C-2), 159.9 (C-3′), 163.4 (d, $^1J_{C-F}$ = 248 Hz, C-4″), 174.8 (C-5′). MS (EI) m/z for $C_{21}H_{24}FN_3O$: 353.2 (M^+, 100%).

4-[3-(4-Fluorophenyl)-5-isopropylisoxazol-4-yl]-*N*-(tetrahydro-2*H*-pyran-4-yl)pyridin-2-amine (7). This compound was obtained according to general procedure from compound **5** (0.3 g, 1 mmol) and tetrahydro-2*H*-pyran-4-amine (0.8 g, 8 mmol). The residue was purified by flash chromatography (SiO_2, eluent: petrol ether 25%/ethyl acetate 75%) to afford the title compound as white solid (37%). Melting point: 117.0 °C. ^{1}H NMR ($CDCl_3$, 200 MHz, ppm): δ (ppm) 1.36 (d, J = 6.84 Hz, 6H, 2 × CH_3), 1.51 (m, 2H, tetrahydro-2*H*-pyran), 1.89 (m, 2H, tetrahydro-2*H*-pyran), 3.19 (m, 1H, $CHMe_2$), 3.47 (m, 2H, tetrahydro-2*H*-pyran), 3.73 (m, 1H, tetrahydro-2*H*-pyran), 3.97 (m, 2H, tetrahydro-2*H*-pyran), 4.49 (d, J = 5.53 Hz, 1H, NH), 6.09 (s, 1H, 4-Pyr), 6.41 (d, J = 4.97 Hz, 1H, 4-Pyr), 7.04 (m, 2H, 4-F-ph), 7.46 (m, 2H, 4-F-ph), 8.09 (d, J = 5.15 Hz, 1H, 4-Pyr). ^{13}C NMR ($CDCl_3$, 200 MHz, ppm): δ (ppm) 20.9 (2 × CH_3), 26.4 (CH), 33.3 (2 × CH_2, tetrahydro-2*H*-pyran), 47.5 (CH, tetrahydro-2*H*-pyran), 66.6 (2 × CH_2, tetrahydro-2*H*-pyran), 107.8 (C-5), 112.2 (C-4′), 113.9 (C-3), 115.7 (d, $^2J_{C-F}$ = 21.8 Hz, C-3″/C-5″), 124.8 (d, $^4J_{C-F}$ = 3.4 Hz, C-1″), 130.3 (d, $^3J_{C-F}$ = 8.4 Hz, C-2″/C-6″), 139.9 (C-4), 148.6 (C-6), 157.8 (C-2), 159.9 (C-3′), 163.4 (d, $^1J_{C-F}$ = 248 Hz, C-4″), 175.6 (C-5′). MS (EI) m/z: 381 (M^+, 28%), 254 (100%). HRMS (EI) for $C_{22}H_{24}FN_3O_2$ (M^+): calcd, 381.18523; found, 381.18187. The compound was proven by X-ray analysis to have the desired structure. For details see Supporting Information. CCDC number: 727846.

4-[3-(4-Fluorophenyl)-5-isopropylisoxazol-4-yl]-*N*-(1(*R*)-phenylethyl)pyridin-2-amine (8). This compound was obtained according to general procedure from compound **5** (0.3 g, 1 mmol) and 1(*R*)-phenylethanamine (1.1 g, 9 mmol). The residue was purified by flash chromatography (SiO_2, eluent: petrol ether 65%/ethyl acetate 35%) to afford the title compound as white solid (36%). Melting point: 119.0 °C. ^{1}H NMR ($CDCl_3$, 200 MHz, ppm): δ (ppm) 1.17 (d, J = 6.98 Hz, 6H, 2 × CH_3), 1.54 (d, J = 6.77 Hz, 3H, CH_3-phenylethanamine), 2.81 (m, 1H, $CHMe_2$), 4.58 (m, 1H, CHMe), 5.23 (d, 1H, NH), 5.98 (s, 1H, 4-Pyr), 6.30 (m, 1H, 4-Pyr), 6.97 (m, 3H, 4-F-ph and phenylethanamine), 7.28−7.38 (m, 6H, 4-F-ph and phenylethanamine), 8.05 (d, J = 4.95 Hz, 1H, 4-Pyr). ^{13}C NMR ($CDCl_3$, 200 MHz, ppm): δ (ppm) 20.8 (2 × CH_3), 24.6 ($CHMe_2$), 26.2 (CH_3), 52.2 (CHMe), 107.2 (C-5), 112.2 (C-4′), 114.3 (C-3), 115.5 (d, $^2J_{C-F}$ = 21.7 Hz, C-3″/C-5″), 124.6 (d, $^4J_{C-F}$ = 3.3 Hz, C-1″), 125.5 (2 × CH_3, ph), 127.0 (CH, ph), 128.6 (2 × CH_3, ph), 130.1 (d, $^3J_{C-F}$ = 8.4 Hz, C-2″/C-6″), 140.1 (C-4), 144.0 (CH, ph), 148.4 (C-6), 158.2 (C-2), 159.7 (C-3′), 163.3 (d, $^1J_{C-F}$ = 248 Hz, C-4″), 174.9 (C-5′). MS (EI) m/z: 401 (M^+, 77%), 386 (100%). HRMS (EI) for $C_{25}H_{24}FN_3O$ (M^+): calcd, 401.19032; found, 401.18846. The compound was proven by X-ray analysis to have the desired structure. For details see Supporting Information. CCDC number: 727847.

4-[3-(4-Fluorophenyl)-5-isopropylisoxazol-4-yl]-*N*-(1(*S*)-phenylethyl)pyridin-2-amine (9). This compound was obtained according to general procedure from compound **5** (0.3 g, 1 mmol) and 1(*S*)-phenylethanamine (1.15 g, 10 mmol). The residue was purified by flash chromatography (SiO_2, eluent: petrol ether 65%/ethyl acetate 35%) to afford the title compound as white solid (37%). Melting point: 120.5 °C. ^{1}H NMR ($CDCl_3$, 200 MHz, ppm): δ (ppm) 1.17 (d, J = 6.98 Hz, 6H, 2 × CH_3), 1.54 (d, J = 6.77 Hz, 3H, CH_3-phenylethanamine), 2.81 (m, 1H, $CHMe_2$), 4.58 (m, 1H, CHMe), 5.18 (d, J = 5.85 Hz 1H, NH), 5.97 (s, 1H, 4-Pyr), 6.30 (m, 1H, 4-Pyr), 6.97 (m, 3H, 4-F-ph and phenylethanamine), 7.28 (m, 6H, 4-F-ph and phenylethanamine), 8.05 (d, J = 5.17 Hz, 1H, 4-Pyr). ^{13}C NMR ($CDCl_3$, 200 MHz, ppm): δ (ppm) 20.8 (2 × CH_3), 24.6 ($CHMe_2$), 26.2 (CH_3), 52.2 (CHMe), 107.2 (C-5), 112.2 (C-4′), 114.3 (C-3), 115.5 (d, $^2J_{C-F}$ = 21.7 Hz, C-3″/C-5″), 124.6 (d, $^4J_{C-F}$ = 3.3 Hz, C-1″), 125.5 (2 × CH_3, ph), 127.0 (CH, ph), 128.6 (2 × CH_3, ph), 130.1 (d, $^3J_{C-F}$ = 8.4 Hz, C-2″/C-6″), 140.1 (C-4), 144.0 (CH, ph), 148.4 (C-6), 158.2 (C-2), 159.7 (C-3′), 163.3 (d, $^1J_{C-F}$ = 248 Hz, C-4″), 174.9 (C-5′). (EI) m/z: 401 (M^+, 77%), 386 (100%). HRMS (EI) for $C_{25}H_{24}FN_3O$ (M^+): calcd, 401.19032; found, 401.19286. The compound was proven by X-ray analysis to have the desired structure. For details see Supporting Information. CCDC number: 727848.

***N*-[4-(3-(4-Fluorophenyl)-5-isopropylisoxazol-4-yl)pyridin-2-yl]acetamide (10).** A mixture of compound **5** (0.15 g, 0.5 mmol), acetamide (0.50 g, 17 mmol), cesium carbonate (0.23 g, 0.7 mmol), Pd_2dba_3 (0.005 g, 0.005 mmol), and Xantphos (0.009 g, 0.016 mmol) was refluxed under argon atmosphere in dioxane (10 mL). The progress of the reaction was followed by TLC. Upon completion of the reaction, the mixture was cooled to rt and partitioned between H_2O and CH_2Cl_2. The aqueous phase was separated and again extracted with CH_2Cl_2. The combined organic layers were dried over Na_2SO_4 and filtered and the solvent removed in vacuo. The oily residue thus obtained was purified by flash chromatography (SiO_2, eluent: petrol ether 50%/ethyl acetate 50%) to afford the title compound as white solid (14%). Melting point: 180 °C. ^{1}H NMR ($CDCl_3$, 200 MHz, ppm): δ (ppm) 1.39 (d, J = 6.98 Hz, 6H, 2 × CH_3), 2.23 (s, 3H, acetamide), 3.25 (m, 1H, $CHMe_2$), 6.73 (m, 1H, 4-Pyr), 7.04 (m, 2H, 4-F-ph), 7.41 (m, 2H, 4-F-ph), 8.20 (d, J = 4.53 Hz, 2H, 4-Pyr), 8.33 (brs, 1H, NH). ^{13}C NMR ($CDCl_3$, 200 MHz, ppm): δ (ppm) 20.8 (2 × CH_3), 24.6 ($CHMe_2$), 26.5 (CH_3, acetamide), 111.8 (C-4′), 114.4 (C-5), 115.7 (d, $^2J_{C-F}$ = 21.7 Hz, C-3″/C-5″), 120.7 (C-3) 124.5 (d, $^4J_{C-F}$ = 3.3 Hz, C-1″), 130.4 (d, $^3J_{C-F}$ = 8.4 Hz, C-2″/C-6″), 141.2 (C-4), 147.7 (C-6), 151.8 (C-2), 159.9

(C-3′), 163.5 (d, $^1J_{C-F}$ = 248 Hz, C-4″, 168.7 (CH, acetamide), 175.5 (C-5′). (EI) *m*/*z*: 339 (M^+, 55%), 296 (100%). HRMS (EI) for $C_{19}H_{18}FN_3O_2$ (M^+): calcd, 339.13828; found, 339.13723.

7-[3-(4-Fluorophenyl)-5-isopropylisoxazol-4-yl]tetrazolo[1,5-*a*]-pyridine (11). Compound **5** (0.7 g, 2.33 mmol) and sodium azide (0.5 g, 7 mmol) were heated in DMSO (5 mL) at 140 °C for 3 h. The title compound precipitated as beige solid upon addition of water to the cold reaction mixture. It was collected by suction filtration, dried, and stored at 5 °C. ^{1}H NMR ($CDCl_3$, 200 MHz, ppm): δ (ppm) 1.42 (d, *J* = 6.97 Hz, 6H, 2 × CH_3), 3.25 (m, 1H, $CHMe_2$), 6.88 (d, *J* = 7.25 Hz, 1H, 4-Pyr), 7.07 (t, *J* = 8.69, 2H, 4-F-ph), 7.40 (m, 2H, 4-F-ph), 8.76 (d, *J* = 7.10 Hz, 1H, 4-Pyr). ^{13}C NMR ($CDCl_3$, 200 MHz, ppm): δ (ppm) 20.9 (2 × CH_3), 26.6 ($CHMe_2$), 110.7 (C-4′), 115.7 (d, $^2J_{C-F}$ = 22.1 Hz, C-3″/C-5″), 116.4 (C-6), 118.5 (C-8), 123.9 (d, $^4J_{C-F}$ = 3.5 Hz, C-1″), 125.2 (C-5), 130.4 (d, $^3J_{C-F}$ = 8.5 Hz, C-2″/C-6″), 135.3 (C-7), 148.7 (C-9), 159.8 (C-3′), 163.7 (d, $^1J_{C-F}$ = 249.6 Hz, C-4″), 176.1 (C-5′).

4-[3-(4-Fluorophenyl)-5-isopropylisoxazol-4-yl]pyridin-2-amine (12). Method A. Compound **11** (0.4 g, 1.24 mmol) and tin(II) chloride dihydrate (1.12 g, 5 mmol) were stirred in methanol (10 mL) at 50 °C for 3 h. The mixture was concentrated, neutralized with sodium hydrogen carbonate and the resulting salt was soaked with water, dichloromethane, and methanol, and the filtrate was evaporated and then extracted by dichloromethane, dried over Na_2SO_4, and evaporated. The residue was purified by flash chromatography (SiO_2, eluent: petrol ether 50%/ethyl acetate 50%) to afford the title compound as yellow solid (54%).

Method B. A stirred solution of compound **11** (0.4 g, 1.24 mmol) in methanol/water (9.5 mL/0.5 mL) was treated with hydrogen gas for 24 h at rt (pressure = 5 bar) in the presence Pd/C (10%) and few drops of conc HCl. The mixture was soaked with methanol (200 mL) and filtered. The filtrate was concentrated, neutralized with sodium hydrogen carbonate, and extracted with dichloromethane. The organic phase was dried over Na_2SO_4 and the solvent was evaporated. The residue was purified by flash chromatography (SiO_2, eluent: petrol ether 25%/ethyl acetate 75%) to afford the title compound as yellow solid (42%). ^{1}H NMR ($CDCl_3$, 200 MHz, ppm): δ (ppm) 1.34 (d, *J* = 6.99 Hz, 6H, 2 × CH_3), 3.18 (m, 1H, $CHMe_2$), 4.59 (brs, 2H, NH_2), 6.29 (s, 1H, 4-Pyr), 6.45 (d, *J* = 3.89 Hz, 1H, 4-Pyr), 7.03 (m, 2H, 4-F-ph), 7.43 (m, 2H, 4-F-ph), 8.06 (d, *J* = 5.13 Hz, 1H, 4-Pyr). ^{13}C NMR ($CDCl_3$, 200 MHz, ppm): δ (ppm) 20.9 (2 × CH_3), 26.4 ($CHMe_2$), 109.1 (C-4′), 112.0 (C-5), 115.6 (d, $^2J_{C-F}$ = 21.7 Hz, C-3″/C-5″), 116.1 (C-3), 124.7 (d, $^4J_{C-F}$ = 3.3 Hz, C-1″), 130.2 (d, $^3J_{C-F}$ = 8.4 Hz, C-2″/C-6″), 140.5 (C-4), 148.5 (C-6), 158.7 (C-2), 159.7 (C-3′), 163.4 (d, $^1J_{C-F}$ = 248.2 Hz, C-4″), 174.9 (C-5′).

2-(4-Fluorophenyl)-*N*-[4-(3-(4-fluorophenyl)-5-isopropylisoxazol-4-yl)pyridin-2-yl]acetamide (13). 2-(4-Fluorophenyl)acetyl chloride (0.072 g, 0.42 mmol) was added under stirring at rt to a solution of compound **12** (0.125 g, 0.42 mmol) in toluene (10 mL). Triethylamine (1 mL) was then added to the mixture, and stirring was continued for 2 h at 80 °C. The reaction mixture was cooled to rt, and aqueous sodium hydrogen carbonate was added. The resulting mixture was finally extracted with ethyl acetate (2 × 30 mL). The combined organic layers were dried over Na_2SO_4 and filtered, and the solvent was removed in vacuo. The oily residue was purified by flash chromatography (SiO_2, eluent: petrol ether 70%/ethyl acetate 30%) to afford the title compound as yellow solid (27%). Melting point: 176 °C. ^{1}H NMR ($CDCl_3$, 200 MHz, ppm): δ (ppm) 1.38 (d, *J* = 6.97 Hz, 6H, 2 × CH_3), 3.23 (m, 1H, CH Me_2),3.74 (s, 2H, 2-(4-F-ph)acetamide), 6.71 (m, 1H, 4-Pyr), 6.98−7.14 (m, 5H, 4-F-ph and 2-(4-F-ph)acetamide), 7.27 (m, 3H, 4-F-ph and 2-(4-F-ph)aetamide), 7.95 (brs, 1H, NH), 8.15−8.20 (m, 2H, 4-Pyr). ^{13}C NMR ($CDCl_3$, 200 MHz, ppm): δ (ppm) 20.8 (2 × CH_3), 26.5 ($CHMe_2$), 43.9 (CH_2), 111.8 (C-4′), 114.3 (C-5), 115.7 (d, $^2J_{C-F}$ = 21.5 Hz, C-3″/C-5″), 116.2 (d, $^2J_{C-F}$ = 11.2 Hz, C-3‴/C-5‴) 120.9 (C-3) 124.5 (d, $^4J_{C-F}$ = 3.4 Hz, C-1″), 129.4 (d, $^4J_{C-F}$ = 3.4 Hz, C-1‴), 130.5 (d, $^3J_{C-F}$ = 8.4 Hz, C-2″/C-6′), 131.0 (d, $^3J_{C-F}$ = 8.1 Hz, C-2‴/C-6‴), 141.2 (C-4), 147.9 (C-6), 151.5 (C-2), 159.8 (C-3′), 162.3 (d, $^1J_{C-F}$ = 241.2 Hz, C-4‴), 163.4 (d, $^1J_{C-F}$ = 248.1 Hz, C-4″), 169.1 (C_q), 175.4 (C-5′). (EI) *m*/*z*: 433 (M^+, 70%), 254 (100%). HRMS (EI) for $C_{25}H_{21}F_2N_3O_2$ (M^+): calcd, 433.160155; found, 433.15855.

***N*-(4-[3-(4-Fluorophenyl)-5-isopropylisoxazol-4-yl]pyridin-2-yl)-2-phenoxypropanamide (14).** 4-(Dimethylamino)pyridine (0.7 g) was added to a solution of 2-phenoxypropanoyl chloride (0.14 g, 0.74 mmol) and compound **12** (0.2 g, 0.67 mmol) in toluene (5 mL). The resulting mixture was stirred for 3 h at 60 °C and then cooled to rt. Aqueous sodium hydrogen carbonate solution was added to the reaction mixture, followed by extraction with CH_2Cl_2 (2 × 20 mL). The organic phase was separated and the combined organic extracts were dried over Na_2SO_4, and the solvent was removed in vacuo. The residue was purified by flash chromatography (SiO_2, eluent: petrol ether 50%/ethyl acetate 50%) to afford the title compound as white solid (50%). Melting point: 105 °C. ^{1}H NMR ($CDCl_3$, 200 MHz, ppm): δ (ppm) 1.41 (m, 6H, 2 × CH_3), 1.67 (d, *J* = 6.75 Hz, 3H, CH_3 (2-phenoxypropanoylamide))3.27 (m, 1H, $CHMe_2$), 4.82 (m, 1H, CH (2-phenoxypropanoylamide)), 6.76 (m, 1H, 4-Pyr), 6.98−7.10 (m, 5H, 4-F-ph and 2-phenoxypropanoylamide), 7.30−7.44 (m, 4H, 4-F-ph and 2-phenoxypropanoylamide), 8.24 (m, 2H, 4-Pyr), 9.04 (brs, 1H, NH). ^{13}C NMR ($CDCl_3$, 200 MHz, ppm): δ (ppm) 18.5 (CH_3), 20.9 (2 × CH_3), 26.5 ($CHMe_2$), 74.9 (CH-phenoxypropanoylamide), 111.7 (C-4′), 114.5 (C-5), 115.5 (2 × CH_3, phenoxy), 115.7 (d, $^2J_{C-F}$ = 21.5 Hz, C-3″/C-5″), 121.1 (C-3), 122.4 (CH, phenoxy), 124.5 (d, $^4J_{C-F}$ = 3.3 Hz, C-1″), 129.6 (2 × CH, phenoxy), 130.4 (d, $^3J_{C-F}$ = 8.4 Hz, C-2″/C-6″), 141.3 (C-4), 147.8 (C-6), 151.1 (C-2), 156.5 (C-1‴, phenoxy), 159.9 (C-3′), 163.5 (d, $^1J_{C-F}$ = 248.1 Hz, C-4″), 171.0 (C_q, CONH), 175.5 (C-5′). (EI) *m*/*z*: 445 (M^+, 5%), 121 (100%). HRMS (EI) for $C_{26}H_{24}FN_3O_3$ (M^+): calcd 445.18014; found 445.18224.

(*E*)-3-(2,4-Dimethoxyphenyl)-*N*-(4-[3-(4-fluorophenyl)-5-isopropylisoxazol-4-yl]pyridin-2-yl)acrylamide (15). To a stirred solution of *trans*-2,4-dimethoxycinnamic acid (0.2 g, 0.96 mmol) in NMP (5 mL) was added CDI (0.16 g, 1.92 mmol). The activation of the acid was controlled by tlc. Upon completion of the reaction, compound **12** (0.14 g, 0.47 mmol) in NMP (2 mL) was added and the reaction mixture heated at 120 °C for 72 h until all of **12** was consumed. The black residue obtained upon evaporation of the solvent was washed with water and extracted with CH_2Cl_2 (2 × 20 mL). The combined organic extracts were dried over Na_2SO_4, and the solvent was removed in vacuo. The residue was purified by flash chromatography (SiO_2, eluent: petrol ether 25%/ethyl acetate 75%) to afford the title compound, which was further purified by preparative thick layer chromatography (Silica Gel 60 F254, 2 mm, eluent: petrol ether 65%/ethyl acetate 35%) to afford the title compound as white solid (18%). Melting point: 221 °C. ^{1}H NMR ($CDCl_3$, 200 MHz): δ (ppm) 1.41 (d, *J* = 6.34 Hz, 6H, 2 × CH_3), 3.26 (m, 1H, CH Me_2) 3.86 (d, *J* = 4.71, 6H, 2 × $-OCH_3$), 6.48−6.70 (m, 4H, 4-Pyr and 3-(2,4-dimethoxyphenyl)acrylamide), 7.04 (m, 2H, 4-F-ph), 7.44 (m, 3H, 4-F-ph and 3-(2,4-dimethoxyphenyl)acrylamide), 7.94 (d, *J* = 16.14 Hz, 1H, −CH (3-(2,4-dimethoxyphenylmac_cpb; acrylamide)), 8.22 (d, *J* = 4.07 Hz, 1H, 4-Pyr), 8.42 (s, 1H, 4-Pyr), 8.60 (brs, 1H, NH). ^{13}C NMR ($CDCl_3$, 200 MHz, ppm): δ (ppm) 20.7 (CH), 26.5 (2 × CH_3), 55.3 (CH_3, $-OCH_3$), 55.4 (CH_3, $-OCH_3$), 98.4 (CH, Ar), 105.2 (CH, Ar), 111.7 (C_q), 114.7 (CH, Ar), 115.7 (d, $^2J_{C-F}$ = 21.7 Hz, C-3″/C-5″), 116.4 (C_q, Ar), 118.3 (CH, CH═CH), 120.4 (CH, Ar), 124.6 (d, $^4J_{C-F}$ = 3.4 Hz, C-1″), 130.4 (d, $^3J_{C-F}$ = 8.4 Hz, C-2″/C-6″), 131.2 (CH, Ar), 139.0 (CH, CH═CH), 141.5(Cq), 147.1 (CH, Ar), 152.4 (C_q), 159.9 (C_q), 160.0 (C_q), 162.7 (C_q), 163.5 (d, $^1J_{C-F}$ = 248.1 Hz, C-4″), 165.4 (C_q), 175.6 (C_q). (EI) *m*/*z*: 487 (M^+, 28%), 191 (100%). HRMS (EI) for $C_{28}H_{26}FN_3O_4$ (M^+): calcd, 487.190701; found, 487.19381.

(*E*)-3-(2,4-Dimethoxy-phenyl)-*N*-(4-[5-(4-fluoro-phenyl)-2-methylsulfanyl-3*H*-imidazol-4-yl]-pyridin-2-yl)-acrylamide (17). (*E*)-2,4-Dimethoxy cinnamic acid (1.25 g, 6.0 mmol) and CDI (1.04 g, 6.4 mmol) were stirred at room temperature in 10 mL of dry DMF for 3 h and 4-[5-(4-fluoro-phenyl)-2-methylsulfanyl-3*H*-imidazol-4-yl]-pyridin-2-ylamine **16** (0.608 g, 2.02 mmol) was added. The mixture was stirred for 10 h at 110 °C. The solvent was removed, and 50 mL of water and 50 mL of ethylacetate were added to the residue. The phases were separated and the organic phase was washed twice with water and once with brine. The solvent was dried over Na_2SO_4, evaporated, and the residue recrystallized from ethyl acetate. Yield: 275 mg (27.7%). Melting point: 225.0 °C. HPLC: 7.97 min, 98.0%. ^{1}H NMR (200 MHz, THF-d_8): δ ppm 2.66 (s, 3 H, $SOCH_3$), 3.81 (s, 3 H, *ortho*-OMe), 3.88 (s, 3 H, *para*-OMe), 6.54 (m, 2 H, Ar.5-H, Ar.3-H), 6.79 (d, J = 15.66 Hz, 1 H, 2-H), 6.95 (m, 1 H, Ar6−H), 7.07 (m, 2H, *meta*-4FPhH), 7.53 (m, 3 H, *ortho*-4FPh-H, Pyr-5-H), 7.88 (d, J = 15.54 Hz, 1 H, 3-H), 8.06 (d, J = 5.31 Hz, 1 H, Pyr-6-H), 8.61 (s, 1 H, Pyr-3-H), 9.55 (s, 1 H, NH). ^{13}C NMR (50.33 MHz, THF-d_8) δ (ppm) 14.1 (S-CH_3), 54.5 (*meta*-OCH_3), 54.6 (*ortho*-OCH_3), 98.0 (CH, Ar), 105.1 (CH, Ar), 110.8 (CH, ArCH), 114.9 (d, 21 Hz, *ortho*-4-FPhH), 116.6 (ArCH), 116.9 (ArCH),119.3 (C═CH-1), 121.2 (CqAr), 129.7 (ArCH), 134.6 (ArCq), 136.6 (Cq), 147.4 (C═CH), 153.4 (Cq), 161.1 (d, 136 Hz, 4FPh−Cq), 164.3 (C═O). MS (ESI) for $C_{26}H_{23}FN_4O_3S$ 591.1 $[M + H]^+$; HRMS calcd 490.14749, found 490.14570.

(*E*)-3-(2,4-Dimethoxy-phenyl)-*N*-(4-[5-(4-fluoro-phenyl)-2-methanesulfinyl-3*H*-imidazol-4-yl]-pyridin-2-yl)-acrylamide (18). Compound **17** (0.176 g, 0.40 mmol) was dissolved in 3.5 mL of THF, and 1 mL of water was added. The mixture was stirred in an ice−water bath for 10 min, and an ice-cold solution of 0.121 g potassium peroxomonosulfate (Oxone) in 2 mL water was added. The mixture was stirred for 2.5 h. After completion of the reaction, 7 mL of sodium hydrogen carbonate solution, 7 mL of water, and 15 mL of EtOAc were added. The phases were separated, and the organic phase washed with water and brine, dried over Na_2SO_4, and evaporated. Yield: 177 mg (91.7%). Melting point: 219.0 °C. HPLC: 7.97 min, 99.9%. ^{1}H NMR (200 MHz, DMSO-d_6) δ ppm: 3.09 (s, 3 H, $SOCH_3$) 3.81 (s, 3 H, *ortho*-OCH_3) 3.87 (s, 3 H, *para*-OCH_3) 6.61 (m, 2 H, Ar.5-H, Ar.3-H) 6.93 (d, J = 15.66 Hz, 1 H, 2-H) 7.03 (dd, J = 5.05 Hz, J = 1.26 Hz 1 H, Pyr-5-H) 7.30 (m, 2 H, *meta*-4FPhH) 7.52 (m, 4 H, *ortho*-4FPhH, Pyr-6-H, *ortho*-ArH) 7.71 (d, J = 15.92 Hz, 1 H, 3-H) 8.22 (m, 1 H, Pyr-3-H) 8.48 (s, 1 H, NH) 10.56* (s, 1 H, imidazoleNH, exchangeable) 13.89* (s, 1 H, imidazoleNH, exchangeable) (*tautomers of imidazole, stabilization by DMSO). ^{13}C NMR (50.33 MHz, THF-D8) δ: (ppm) 40.2 ($SOCH_3$), 54.5 (*meta*-OCH_3), 54.7 (*ortho*-OCH_3), 98.0 (CH, Ar), 105.1 (CH, Ar), 115.1 (d, *ortho*-4FPhC), 116.9 (CH, Ar), 119.2 (C═CH-1), 129.8 (Ar, CH), 136.8 (Cq), 147.5 (C═CH-2), 153.4 (Cq), 161.1 (d, J = 136.95, 4FPh−Cq), 164.3 (C═O). MS (ESI) for $C_{26}H_{23}FN_4O_4S$: 507.1 $[M + H]^+$; HRMS calcd 504.126716, found 504.12372.

Molecular Modeling. All modeling was performed on a Fedora Core 9 Linux system. For visualization and building the structures, Maestro (version 8.5) from Schrodinger (Schrodinger, LLC, New York, NY, 2008) was used (for PDB codes and references, see Figures). The illustrations of modeling were generated by PyMol. Docking studies were performed using the Induced fit docking tool from Schrodinger (Schrodinger Suite 2008 Induced Fit Docking protocol; Glide version 5.0, Schrodinger, LLC, New York, NY, 2005; Prime version 1.7, Schrodinger, LLC, New York, NY, 2005). Chain B from CK1 structure (with CK1δ-specific inhibitor IC261 as original ligand, PDB code 1EH4_B)[9] was used for docking studies such as Homologue, because no suitable structure of mammalian CK1 was available. However, to correlate the model with biological assay data of this study, key amino acids were mutated to residues obtained from rat sequence: I85M, D86E, and L96F. Residue F96 is not involved in active site. The side chain of E86 is situated in the backbone and not affecting the binding mode of compounds. However, the "gatekeeper" residue M85 is significantly important for the binding mode of compounds. For clarity, the unliganded ATP-site of CK1δ structure (PDB 1CKI[24]) was not suitable for modeling experiments in this study.

Biological Evaluation. Inhibitor Solutions. All inhibitor solutions were prepared freshly in DMSO prior to each experiment and used immediately. Inhibitor solutions were light sensitive and thus should be handled under light protection.

Plasmids. For the expression of rat CK1δ as GST- CK1δ fusion protein the plasmid pGEX-2T (449) was used.[31] The plasmid pGEX-2T-CK1$\delta^{1-428/M82F}$ containing a mutation at amino acid 82 (met → phe, "gatekeeper") of rat CK1δ was constructed using the QuikChange site-directed mutagenesis kit according to manufacturers' instructions (Stratagene, La Jolla, USA). The plasmid pGEX-2T-CK1δ^{1-428} (449) served as template and the complementary primers used were 5′-tacaatgtcatggtgtttgagctactgggacccagcctg-3′ (5′ primer) and 5′-atgttacagtaccacaaactcgatgaccctgggtcggac-3′ (3′ primer).

Cell Lines. Cell line AC1-M88 was used for cell culture experiments. AC1-M88 cells were generated by fusion of extravillous trophoblasts with AC1−1, a mutant of the choriocarcinoma cell line Jeg-3.[35] AC1-M88 cells were grown in DMEM/F-12 medium (Gibco, Karlsruhe, Germany) supplemented with 10% fetal calf serum (FCS; Gibco, Karlsruhe, Germany) at 37 °C in a humidified 5% CO_2 atmosphere. Cells were treated with various potential CK1 kinase inhibitors as indicated and used for flow cytometry. Control cells were treated with DMSO.

Flow Cytometry/FACS Analysis. For discrimination of living and dead cells, cells were washed twice with PBS and resuspended in PBS containing propidium iodide. After 10 min incubation FACS analyses were performed. Unstained cells were regarded as living cells. For cell cycle analyses the "Cycle Test Plus Kit" (Becton Dickinson, USA) was used according to the manufacturer's protocol and cells were analyzed using the Becton Dickinson "FACScan" flow cytometer and the "Cell Quest" software.

Overexpression and Purification of Glutathione *S*-Transferase Fusion Proteins. The production and purification of the GST-fusion proteins FP267, FP449, and GST-CK1$\delta^{1-428/M82F}$ were carried out as described elsewhere.[30] CK1δkd was purchased from NEB (Ipswich, USA), CK1ε from Invitrogen (Karlsruhe, Germany).

In Vitro Kinase Assays. In vitro kinase assays were carried out in presence of various potential inhibitors of CK1δ at an ATP concentration of 0.1 mM and DMSO control as described previously.[31] In some cases ATP was used in concentrations of 0.05, 0.25, or 0.5 mM. Compounds **21** (IC261)[9] and D4467[11,12] have been reported to inhibit CK1δ and were used as positive controls. The GST-p53$^{1-64}$ fusion protein (FP267) was used as substrate. Recombinant CK1δ kinase domain (CK1δkd, NEB, Ipswich, USA), GST-CK1δ (FP449) and recombinant CK1ε (Invitrogen, Karlsruhe, Germany) were used as sources of the enzyme. Phosphorylated proteins were separated by SDS-PAGE and the protein bands were visualized on dried gels by autoradiography. The phosphorylated protein bands were excised and quantified by Cherenkov counting.

Acknowledgment. We thank Barbara Radunsky and Arnhild Grothey, Department of General, Visceral, and Transplantation Surgery, University of Ulm, for excellent technical support. We thank Jenny Moran for screening of compounds in the kinase profiler at the Division of Signal Transduction Therapy, University of Dundee. We thank Dr. D. Schollmeyer for X-ray analysis of compounds. Financial support by DAAD, Deutsche Forschungsgemeinschaft, and Merckle GmbH, Blaubeuren, is gratefully acknowledged. Work in

the lab of Uwe Knippschild is supported by Deutsche Krebshilfe, Mildred Scheel Stiftung (108489).

Supporting Information Available: Experimental and spectroscopic details for compounds **3**, **4**, and **5**. IR-data and purity of key target compounds. X-ray analysis for compounds **1**, **2**, **7**, **8** and **9**. Assay details and ATP concentrations. This material is available free of charge via the Internet at http://pubs.acs.org.

References

(1) Zhang, J.; Yang, P. L.; Gray, N. S. Targeting cancer with small molecule kinase inhibitors. *Nat. Rev. Cancer* **2009**, *9*, 28–39.

(2) Peifer, C.; Kinkel, K.; Abadleh, M.; Schollmeyer, D.; Laufer, S. From Five- to Six-Membered Rings: 3,4-Diarylquinolinone as Lead for Novel p38MAP Kinase Inhibitors. *J. Med. Chem.* **2007**, *50*, 1213–1221.

(3) Peifer, C.; Urich, R.; Schattel, V.; Abadleh, M.; Rottig, M.; Kohlbacher, O.; Laufer, S. Implications for selectivity of 3,4-diarylquinolinones as p38αMAP kinase inhibitors. *Bioorg. Med. Chem. Lett.* **2008**, *18*, 1431–1435.

(4) Peifer, C.; Wagner, G.; Laufer, S. New approaches to the treatment of inflammatory disorders small molecule inhibitors of p38 MAP kinase. *Curr. Top. Med. Chem.* **2006**, *6*, 113–149.

(5) Godl, K.; Wissing, J.; Kurtenbach, A.; Habenberger, P.; Blencke, S.; Gutbrod, H.; Salassidis, K.; Stein-Gerlach, M.; Missio, A.; Cotten, M.; Daub, H. An efficient proteomics method to identify the cellular targets of protein kinase inhibitors. *Proc. Natl. Acad. Sci. U.S.A.* **2003**, *100*, 15434–15439.

(6) Bain, J.; Plater, L.; Elliott, M.; Shpiro, N.; Hastie, C. J.; McLauchlan, H.; Klevernic, I.; Arthur, J. S. C.; Alessi, D. R.; Cohen, P. The selectivity of protein kinase inhibitors: A further update. *Biochem. J.* **2007**, *408*, 297–315.

(7) Shanware, N. P.; Williams, L. M.; Bowler, M. J.; Tibbetts, R. S. Nonspecific in vivo inhibition of CK1 by the pyridinyl imidazole p38 inhibitors SB 203580 and SB 202190. *BMB Rep.* **2009**, *42*, 142–147.

(8) Laufer, S.; Thuma, S.; Peifer, C.; Greim, C.; Herweh, Y.; Albrecht, A.; Dehner, F. An immunosorbent, nonradioactive p38 MAP kinase assay comparable to standard radioactive liquid-phase assays. *Anal. Biochem.* **2005**, 135–137.

(9) Mashhoon, N.; DeMaggio, A. J.; Tereshko, V.; Bergmeier, S. C.; Egli, M.; Hoekstra, M. F.; Kuret, J. Crystal structure of a conformation-selective casein kinase-1 inhibitor. *J. Biol. Chem.* **2000**, *275*, 20052–20060.

(10) Chijiwa, T.; Hagiwara, M.; Hidaka, H. A newly synthesized selective casein kinase I inhibitor, *N*-(2-aminoethyl)-5-chloroisoquinoline-8-sulfonamide, and affinity purification of casein kinase I from bovine testis. *J. Biol. Chem.* **1989**, *264*, 4924–4927.

(11) Rena, G.; Bain, J.; Elliott, M.; Cohen, P. D4476, a cell-permeant inhibitor of CK1, suppresses the site-specific phosphorylation and nuclear exclusion of FOXO1a. *EMBO Rep.* **2004**, *5*, 60–65.

(12) Cozza, G.; Gianoncelli, A.; Montopoli, M.; Caparrotta, L.; Venerando, A.; Meggio, F.; Pinna, L. A.; Zagotto, G.; Moro, S. Identification of novel protein kinase CK1 delta (CK1delta) inhibitors through structure-based virtual screening. *Bioorg. Med. Chem. Lett.* **2008**, *18*, 5672–5675.

(13) Gross, S. D.; Anderson, R. A. Casein kinase I: Spatial organization and positioning of a multifunctional protein kinase family. *Cellular Signalling* **1998**, *10*, 699–711.

(14) Kritikou, E. Cell signalling: fill in the Wnt gaps. *Nat. Rev. Mol. Cell Biol.* **2006**, *7*, 82.

(15) Budini, M.; Jacob, G.; Jedlicki, A.; Perez, C.; Allende, C. C.; Allende, J. E. Autophosphorylation of carboxy-terminal residues inhibits the activity of protein kinase CK1alpha. *J. Cell. Biochem.* **2008**, *106*, 399–408.

(16) Knippschild, U.; Gocht, A.; Wolff, S.; Huber, N.; Lohler, J.; Stoter, M. The casein kinase 1 family: participation in multiple cellular processes in eukaryotes. *Cell. Signalling* **2005**, *17*, 675–689.

(17) Knippschild, U.; Wolff, S.; Giamas, G.; Brockschmidt, C.; Wittau, M.; Wurl, P. U.; Eismann, T.; Stoter, M. The role of the casein kinase 1 (CK1) family in different signaling pathways linked to cancer development. *Onkologie* **2005**, *28*, 508–514.

(18) Flajolet, M.; He, G.; Heiman, M.; Lin, A.; Nairn, A. C.; Greengard, P. Regulation of Alzheimer's disease amyloid-beta formation by casein kinase I. *Proc. Natl. Acad. Sci. U.S.A.* **2007**, *104*, 4159–4164.

(19) Aud, D. M.; Peng, S. L.-Y. Methods of treating inflammatory diseases with selective inhibitors of the casein kinase 1 isoforms. [*F. Hoffmann-La Roche A.-G.*]. Patent WO. 2007-EP63339[2008071605] 2007.

(20) Giamas, G.; Stebbing, J.; Vorgias, C. E.; Knippschild, U. Protein kinases as targets for cancer treatment. *Pharmacogenomics* **2007**, *8*, 1005–1016.

(21) Green, J.; Bemis, G.; Grillot, A.-L.; Ledeboer, M.; Salituro, F.; Harrington, E.; Gao, H.; Baker, C.; Cao, J.; Hale, M. Preparation of as isoxazolylpyrimidines and related compounds as inhibitors of c-JUN N-terminal kinases and other protein kinases. *PCT Int. Appl. WO 200101262196*, 2001.

(22) Golebiowski, A.; Townes, J. A.; Laufersweiler, M. J.; Brugel, T. A.; Clark, M. P.; Clark, C. M.; Djung, J. F.; Laughlin, S. K.; Sabat, M. P.; Bookland, R. G. The development of monocyclic pyrazolone based cytokine synthesis inhibitors. *Bioorg. Med. Chem. Lett.* **2005**, *15*, 2285–2289.

(23) Wang, Z.; Canagarajah, B. J.; Boehm, J. C.; Kassisa, S.; Cobb, M. H.; Young, P. R.; Abdel-Meguid, S.; Adams, J. L.; Goldsmith, E. J. Structural basis of inhibitor selectivity in MAP kinases. *Structure* **1998**, *6*, 1117–1128.

(24) Longenecker, K. L.; Roach, P. J.; Hurley, T. D. Three-dimensional structure of mammalian casein kinase I: molecular basis for phosphate recognition. *J. Mol. Biol.* **1996**, *257*, 618–631.

(25) Thaher, B. A.; Koch, P.; Schattel, V.; Laufer, S. Role of the Hydrogen Bonding Heteroatom-Lys53 Interaction between the p38α Mitogen-Activated Protein (MAP) Kinase and Pyridinyl-Substituted 5-Membered Heterocyclic Ring Inhibitors. *J. Med. Chem.* **2009**, *52*, 2613–2617.

(26) Liverton, N. J.; Butcher, J. W.; Claiborne, C. F.; Claremon, D. A.; Libby, B. E.; Nguyen, K. T.; Pitzenberger, S. M.; Selnick, H. G.; Smith, G. R.; Tebben, A.; Vacca, J. P.; Varga, S. L.; Agarwal, L.; Dancheck, K.; Forsyth, A. J.; Fletcher, D. S.; Frantz, B.; Hanlon, W. A.; Harper, C. F.; Hofsess, S. J.; Kostura, M.; Lin, J.; Luell, S.; O'Neill, E. A.; Orevillo, C. J.; Pang, M.; Parsons, J.; Rolando, A.; Sahly, Y.; Visco, D. M.; O'Keefe, S. J. Design and synthesis of potent, selective, and orally bioavailable tetrasubstituted imidazole inhibitors of p38 mitogen-activated protein kinase. *J. Med. Chem.* **1999**, *42*, 2180–2190.

(27) Yin, J.; Buchwald, S. L. Pd-Catalyzed Intermolecular Amidation of Aryl Halides: The Discovery that Xantphos Can Be Trans-Chelating in a Palladium Complex. *J. Am. Chem. Soc.* **2002**, *124*, 6043–6048.

(28) Angibaud, P.; Mevellec, L.; Meyer, C.; Bourdrez, X.; Lezouret, P.; Pilatte, I.; Poncelet, V.; Roux, B.; Merillon, S.; End, D. W.; Van Dun, J.; Wouters, W.; Venet, M. Impact on farnesyltransferase inhibition of 4-chlorophenyl moiety replacement in the Zarnestra series. *Eur. J. Med. Chem.* **2007**, *42*, 702–714.

(29) Fisher, M. H. Preparation of morpholine derivatives as animal growth promoters, bronchodilators, antidepressants, and antiobesity agents. [*Merck and Co., Inc.*]. U.S. Patent US. 90-597976[5077290], 10, 1990.

(30) Wolff, S.; Xiao, Z.; Wittau, M.; Suessner, N.; Stoeter, M.; Knippschild, U. Interaction of casein kinase 1 delta (CK1delta) with the light chain LC2 of microtubule associated protein 1A (MAP1A). *Biochim. Biophys. Acta, Mol.Cell Res.* **2005**, *1745*, 196–206.

(31) Knippschild, U.; Milne, D.; Campbell, L.; Meek, D. p53 N-terminus-targeted protein kinase activity is stimulated in response to wild type p53 and DNA damage. *Oncogene* **1996**, *13*, 1387–1393.

(32) Xu, R.-M.; Carmel, G.; Sweet, R. M.; Kuret, J.; Cheng, X. Crystal structure of casein kinase-1, a phosphate-directed protein kinase. *EMBO J.* **1995**, *14*, 1015–1023.

(33) Laufer, S. A.; Hauser, D. R. J.; Domeyer, D. M.; Kinkel, K.; Liedtke, A. J. Design, Synthesis, and Biological Evaluation of Novel Tri- and Tetrasubstituted Imidazoles as Highly Potent and Specific ATP-Mimetic Inhibitors of p38 MAP Kinase: Focus on Optimized Interactions with the Enzyme's Surface-Exposed Front Region. *J. Med. Chem.* **2008**, *51*, 4122–4149.

(34) Stoter, M.; Bamberger, A.; Aslan, B.; Kurth, M.; Speidel, D.; Loning, T.; Frank, H.; Kaufmann, P.; Lohler, J.; Henne-Bruns, D.; Deppert, W.; Knippschild, U. Inhibition of casein kinase I delta alters mitotic spindle formation and induces apoptosis in trophoblast cells. *Oncogene* **2005**, *24*, 7964–7975.

(35) Frank, H. G.; Gunawan, B.; Ebeling-Stark, I.; Schulten, H. J.; Funayama, H.; Cremer, U.; Huppertz, B.; Gaus, G.; Kaufmann, P.; Fuzesi, L. *Cancer Genet. Cytogenet.* **2000**, *116*, 16–22.